Title: Enhancing KCC2 function reduces interictal activity and prevents seizures in mesial temporal lobe epilepsy

Authors: Florian Donneger[1,2,3], Adrien Zanin[1,2,3], Jeremy Besson[1,2,3], Yoness Kadiri[1,2,3], Carla Pagan[1,2,3], Nicolas David[1,2,3], Marion Russeau[1,2,3], Franck Bielle[2,4,5], Bertrand Devaux[6†], Bertrand Mathon[2,5,7], Vincent Navarro[2,5,7], Francine Chassoux[6†], Jean Christophe Poncer[1,2,3]*

Affiliations:

[1] Inserm UMR-S 1270; Paris, France

[2] Sorbonne Université; Paris, France

[3] Institut du Fer à Moulin; Paris, France

[4] AP-HP, Hôpitaux Universitaires La Pitié Salpêtrière - Charles Foix, Department of Neuropathology, F-75013; Paris, France

[5] Paris Brain Institute, INSERM, CNRS; Paris, France,

[6] Department of Neurosurgery, Sainte-Anne Hospital; Paris, France

[7] AP-HP, Epilepsy Unit, Reference Center for Rare Epilepsies, and Department of Clinical Neurophysiology, Pitié Salpêtrière Hospital; Paris, France

*Corresponding author: Jean Christophe Poncer, Institut du Fer à Moulin, 8 rue des Fossés Saint Marcel, 75005 Paris, France. Tel. +33145876118, E-mail: jean-christophe.poncer@inserm.fr

† Present address: Neurosurgery Department, Lariboisière Hospital; Paris, France.

Abstract: The neuronal K/Cl cotransporter KCC2 controls intraneuronal chloride and subsequently the efficiency of GABA signaling. In many neurological disorders, including mesial temporal lobe epilepsy (mTLE), reduced KCC2 expression or function may lead to depolarizing GABA signaling, which may then contribute to pathological activity and seizures. Compensating for the dysregulation of chloride transport in the pathology therefore appears to be a promising therapeutic strategy. Two small molecules - prochlorperazine (PCPZ) and CLP-257 - recently identified from library screening as candidate KCC2 enhancers, appear to improve symptoms in animal models of disorders associated with KCC2 extinction. However, their mode of action in cortical neurons and their therapeutic potential in epilepsy remain elusive and even controversial. Here, we show in rat hippocampal neurons that PCPZ and CLP-257 act by increasing KCC2 function and clustering while decreasing its membrane diffusion, independent of phosphorylation of canonical regulatory residues. Consistently, both compounds suppress spontaneous interictal-like discharges in postoperative tissue from patients with mTLE. Chronic administration of PCPZ also reduces seizure frequency and interictal activity in a mouse model of mTLE. These results unravel the mechanism of action of two KCC2 enhancers and validate their therapeutic potential in mesial temporal lobe epilepsy.

Introduction

Epilepsy is among the most frequent neurological disorders, affecting more than 65 million people worldwide *(1)*. Mesial temporal lobe epilepsy (mTLE), the most common form of focal epilepsy in adults, is frequently associated with hippocampal sclerosis and often refractory to antiseizure medication *(2)*. Surgical resection of the epileptic focus has been shown to offer a fairly high rate (60-75%) of seizure control at 2 years in patients with mTLE *(3)*. However, surgery cannot be proposed to all patients with mTLE. In addition, it can have negative effects on cognitive functions and fewer than 50% remain seizure-free 10 years after surgery *(4)*, highlighting the need for novel therapeutic approaches in mTLE.

Several forms of pharmaco-resistant epilepsies, including mTLE, have been associated with altered expression and function of cation-chloride cotransporters (CCCs), which control transmembrane chloride gradients *(5–10)*. In neurons specifically, the potassium-chloride cotransporter KCC2 maintains a low intracellular chloride concentration, thereby ensuring a hyperpolarizing and inhibitory current upon activation of the chloride-permeable $GABA_A$ receptors *(11)*. Reduced KCC2 expression and function, as often reported in mTLE *(7, 9, 12)* but see *(13)*, leads to elevated intraneuronal chloride and may reduce or even reverse the driving force for $GABA_A$ receptors *(7, 14, 15)*. Depolarizing and excitatory GABA signaling may then paradoxically enhance neuronal activity and is thought to promote anomalous synchronization underlying epileptiform activities *(16–18)*. Thus, pharmacologically rescuing intraneuronal chloride using bumetanide, an antagonist of the chloride importer NKCC1, suppresses interictal-like activity in resective human temporal lobe tissue *in vitro (7)*. Similarly, mutations that promote KCC2 membrane stability and function *(19)* or overexpression of recombinant KCC2

(20) reduced acute seizures in animal models. Compensating for CCC dysfunction therefore appears as a promising therapeutic strategy in pharmacoresistant epilepsy.

Bumetanide, however, failed to prevent acute neonatal seizures in two clinical trials and induced several side-effects due to the broad peripheral NKCC1 expression *(21, 22)*. Instead, enhancing the function of the neuron-specific chloride extruder KCC2 is expected to rescue neuronal chloride transport in the pathology with fewer side effects. Recently, high-throughput screening studies of compound libraries have identified the phenothiazine-derived antipsychotic prochlorperazine (PCPZ) and the arylmethylidine family compounds CLP-257 and CLP290, as enhancers of KCC2 function in heterologous cell lines *(23, 24)*. These compounds were also reported to improve symptoms in animal models of disorders associated with reduced KCC2 expression *(24–28)*. However, their mode of action remains unknown and their efficacy and selectivity towards KCC2 were recently disputed *(29, 30)*. In addition, CLP-257 was shown to either increase *(31)* or decrease *(32)* the duration of epileptiform discharges *in vitro*, and direct experimental evidence of the therapeutic efficacy of KCC2 enhancers in mTLE is missing.

Here, we first investigated the efficacy and mode of action of PCPZ and CLP-257 on KCC2 in rat hippocampal neurons. We show that both compounds enhance KCC2 function and that CLP-257 additionally acts as a positive allosteric modulator of extrasynaptic but not synaptic $GABA_A$ receptors. Both PCPZ and CLP-257 reduced KCC2 membrane diffusion and enhanced KCC2 clustering, without affecting total or plasmalemmal KCC2 expression levels, or phosphorylation of its canonical regulatory residues. *In vitro*, both KCC2 enhancers effectively suppressed spontaneous, interictal-like discharges in postoperative tissue from mTLE patients. Finally, chronic PCPZ administration reduced the occurrence of seizures and other epileptiform activities

in a lithium-pilocarpine mouse model of mTLE. Collectively, our data confirm the efficacy and decipher the mode of action of two candidate KCC2 enhancers, and demonstrate for the first time their antiepileptic potential in a form of pharmacoresistant epilepsy.

Results

PCPZ and CLP-257 act as KCC2 enhancers in rat hippocampal neurons

We first tested whether PCPZ and CLP-257, two candidate KCC2 enhancers *(23, 24)*, potentiate KCC2 in rat hippocampal neurons *in vitro*. KCC2 function was assessed by measuring the somato-dendritic gradient of the reversal potential of currents evoked by focal $GABA_A$ receptor activation (E_{GABA}) in whole-cell recordings with high-chloride internal solution (**Fig. 1**, see Supplementary Material and Methods). As shown in previous studies, this gradient is nearly abolished by a specific KCC2 antagonist *(33, 34)*, but unaffected by bumetanide *(35)*, therefore providing a reliable proxy for KCC2 function. We performed a 2-hour treatment with CLP-257 or PCPZ, a paradigm used in previous studies with CLP-257 *(23, 36)*. The mean somato-dendritic E_{GABA} gradient (Δ_{EGABA}) was 6.6±0.8 mV/100 µm in control neurons (DMSO; n=19). In neurons pre-incubated with PCPZ (10 µM), this gradient was significantly increased to 11.5±1.5 mV/100 µm (n=16; p=0.006; **Fig. 1, A** to **C**). Similarly, pre-incubation with CLP-257 (100 µM) increased ΔE_{GABA} from 5.3±1.1 to 9.7±1.1 mV/100 µm (n=10 and 8, respectively; p=0.014) (**Fig. 1, D** to **F**). Neither compound had an effect on neuronal membrane resistance or series resistance (Fig. S1). These data demonstrate that both PCPZ and CLP-257 effectively potentiate KCC2 function in rat hippocampal neurons.

CLP-257 but not PCPZ directly modulates $GABA_A$ receptor function

CLP-257 has been suggested to act directly to potentiate $GABA_A$ receptors *(29)* (but see *(30)*). Because $GABA_A$ receptor-mediated chloride fluxes modulate KCC2 membrane expression and function *(37)*, we asked whether PCPZ and CLP-257 may act primarily to modulate $GABA_A$

receptor function. We therefore tested their effect on $GABA_A$ receptor-mediated currents, using focal application of isoguvacine (100 µM) or uncaging of low concentration (30 µM) of Rubi-GABA, respectively (**Fig. 2**). PCPZ had no significant effect on the amplitude (157.5±25.4 vs. 150.7±17.5 pA for control, p=0.48) or decay time constant (130.8±10.5 vs. 127.7±10.2 ms, p=0.362) of $GABA_A$ receptor-mediated currents (**Fig. 2, A** to **B**). In contrast, CLP-257 rapidly increased their decay time constant (218.2±21.1 vs. 124.4±9.1 ms, p<0.001) with no detectable effect on their amplitude (162.0±6.6 vs 164.7±4.6 pA for control, p=0.66; **Fig. 2, C** to **D**). The effect of CLP-257 did not appear to be dose-dependent, as previously suggested *(30)*, since application of a 10-fold lower concentration (10 µM) similarly increased the decay time constant of $GABA_A$ receptor-mediated currents (294.1±33.8 vs. 239.7±27.2 ms, p<0.001; Fig. S2).

We next tested the effect of PCPZ and CLP-257 specifically on synaptic $GABA_A$ receptors, by recording miniature inhibitory postsynaptic currents (mIPSCs) from hippocampal neurons. Neither PCPZ nor CLP-257 had detectable effects on mIPSC amplitude (42.9±2.6 vs. 42.5±2.5 pA, p=0.797 and 43.8±2.9 vs. 42.3±3.4 pA, p=0.622, respectively) or decay time constant (10.2±0.7 vs. 10.7±0.8 ms, p=0.086 and 12.5±1.0 vs. 12.4±0.8 ms, p=0.86, respectively). Taken together, these results demonstrate that while both PCPZ and CLP-257 potentiate KCC2 function, CLP-257 also acts to specifically potentiate high-affinity, presumably extrasynaptic but not synaptic $GABA_A$ receptor function in a benzodiazepine-like manner in rat hippocampal neurons.

PCPZ and CLP-257 promote KCC2 membrane confinement and clustering without affecting its total or plasmalemmal expression levels

We then investigated the mechanisms underlying the potentiation of KCC2 by PCPZ and CLP-257. Enhancement of KCC2 function may result from either an increase in intrinsic enzymatic activity, an increase in membrane expression of the transporter, or both *(38)*. We therefore used surface biotinylation to test whether PCPZ or CLP-257 influenced plasmalemmal KCC2 expression. Incubation with PCPZ or CLP-257 for 2 hours had no significant effect on total KCC2 expression (**Fig. 3A**, p=0.137 and p=0.893, respectively) or on the ratio of surface to total expression (**Fig. 3B**, p=0.735 and p=0.8, respectively). Therefore, enhanced KCC2 function by PCPZ or CLP-257 does not reflect an increased expression of the transporter. PCPZ and CLP-257 also had no effect on total NKCC1 expression (p=0.100 and p=0.700, respectively) or on the ratio of surface to total NKCC1 expression (p=0.700 and p=0.700, respectively; Fig. S3).

KCC2 function is regulated by fine tuning of its diffusion and clustering properties at the plasma membrane *(39)*. Thus, the potentiation of KCC2 function is often associated with decreased membrane diffusion and increased clustering *(37, 40–42)*. Membrane lateral diffusion of recombinant Flag-tagged KCC2 was assessed in hippocampal neurons using single particle tracking with quantum dots. The lateral diffusion of KCC2 was reduced by both PCPZ and CLP-257, both in the vicinity of GABAergic synapses and outside. Thus, both compounds reduced the diffusion coefficient of recombinant KCC2 (extrasynaptic: -36.5±14.9% p<0.001; synaptic: -26.2±14.0% p=0.011 for PCPZ and extrasynaptic: -20.7±4.9% p=0.003; synaptic: +9.4±11.2% p=0.97 for CLP-257) as well as its explored area (extrasynaptic: -39.7±17.2% p<0.001; synaptic: -30.6±25.4% p<0.001 for PCPZ and extrasynaptic: -25.1±2.7% p<0.001; synaptic: +4.9±19.4% p=0.80 for CLP-257; **Fig. 3, C** to **D**).

This effect was associated with an increase in KCC2 clustering, as shown by immunocytochemistry assays revealing an increase in cluster intensity (+109.0±61.4% $p<0.001$ and +33.9±13.6% $p=0.005$, respectively) and area (+45.3±18.1% $p<0.001$ and +36.3±20.4% $p<0.001$, respectively), without significant change in cluster density (-6.6±8.4% $p=0.13$ and -3.5±4.2% $p=0.34$; **Fig. 3, E** to **F**). Furthermore, the effect of PCPZ on KCC2 clustering did not involve D2R antagonism, as a 2-hour treatment with eticlopride did not significantly affect the intensity, area, or density of KCC2 clusters (Fig. S4).

Overall, our results demonstrate that PCPZ and CLP-257 act to enhance net KCC2 function and promote its clustering, with no effect on total or plasmalemmal KCC2 expression levels. Therefore, PCPZ and CLP-257 likely induce a redistribution of membrane-inserted KCC2, resulting in increased clustering and function.

PCPZ and CLP-257 do not affect KCC2 phosphorylation on canonical regulatory residues

The stability, clustering, and membrane turnover of KCC2 are controlled by a variety of post-translational mechanisms, including phosphorylation of key residues, particularly in its large carboxy-terminal domain, that regulate its net transport function *(38, 39, 43)*. Phosphorylation of serine 940 (S940) by protein kinase C is known to increase the membrane stability and function of KCC2 *(40, 44)*. In contrast, phosphorylation of threonine residues 906 and 1007 (T906, T1007) by the With-no-lysine (WNK) kinase pathway has been shown to negatively regulate KCC2 function in cortical neurons by affecting its membrane diffusion and clustering *(37, 45)*. We therefore asked whether PCPZ and CLP-257 could act by modulating the phosphorylation of these residues to promote KCC2 function. Immunoprecipitation assays on hippocampo-cortical

slices from adult rats (**Fig. 4, A** to **B**, see Supplementary Material and Methods) revealed no significant effect of PCPZ or CLP-257 on KCC2 phosphorylation at either S940 (-19.7±34.4%, p=0.597 and +20.3±18.7%, p=0.339), T1007 (-18.5±17.1%, p=0.340 and +26.4%±17.0% p=0.195 respectively) or T906 residues (-12.7±10.9%, p=0.308 and -10.2±10.4%, p=0.384 respectively). Consistent with these results, PCPZ and CLP-257 also had no significant effect on the phosphorylation of the WNK effectors SPAK (S373, +33.3±24.0%, p=0.238 and +36.9±48.4%, p=0.488 respectively) and OSR1 (S325, +11.5±18.5%, p=0.568 and +11.8±23.5%, p=0.641, respectively) or their total expression levels (SPAK, -6.0±17.4%, p=0.748 and -12.3±6.4%, p=0.124, respectively; OSR1, -2.2 ±8.3%, p=0.800 and +26.3±12.8%, p=0.108, respectively; **Fig. 4, C** to **D**). In contrast, the pan-WNK inhibitor WNK463 *(46)* reduced phosphorylation of T1007 (-78.7 ±3.3%, p<0.001) and to a lesser extent S940 (-14.4±4.7%, p=0.037) but not T906 (-13.7 ±12.5%, p=0.333; **Fig. 4, A** to **B**). These effects of WNK463 were associated with reduced phosphorylation of SPAK (S373, -84.1±4.6%, p<0.001) and OSR1 (S325, -81.0±5.6%, p<0.001; **Fig. 4, C** to **D**). Thus, PCPZ and CLP-257 appear to potentiate KCC2 clustering and function independent of detectable changes in phosphorylation of serine 940 and threonine 906 and 1007 residues. Consistent with this conclusion, these compounds showed no direct inhibitory effect on the activity of WNK1, WNK3, SPAK or OSR1 in *in vitro* kinase assays (Fig. S5).

Finally, phosphorylation of residues Y903 and Y1087 has been reported to affect KCC2 clustering and function *(42, 47)*. Therefore, we tested the effect of PCPZ and CLP-257 on KCC2 tyrosine phosphorylation in hippocampo-cortical slices from adult rats (**Fig. 4, E** to **F**). Whereas sodium orthovanadate (Na3VO4), a tyrosine phosphatase inhibitor, increased tyrosine

phosphorylation of KCC2 (+89.1±45.4%, p=0.029), PCPZ and CLP-257 showed no significant effect (+6.4±14.7% and +19.0±15.0%, p=1 and p=0.343, respectively). Together, our results demonstrate that PCPZ and CLP-257 potentiate KCC2 function, reduce its diffusion and increase its clustering via a mechanism independent of phosphorylation of canonical regulatory residues in its carboxy-terminal domain.

PCPZ and CLP-257 prevent spontaneous interictal-like activity in postoperative tissue from mTLE patients *in vitro*

Human epileptic tissue therapeutically resected from patients diagnosed with mTLE provides an invaluable tool for evaluating antiepileptic drug candidates in the pathophysiological context of human mTLE *(48, 49)*. We therefore tested the effect of PCPZ and CLP-257 on 13 tissue samples resected from patients diagnosed with mTLE, 11 of which were associated with hippocampal sclerosis (HS) (**Table 1**). As previously reported *(6, 7)*, a majority of slices (29/46) prepared from 13 postoperative tissues and recorded using multi-electrode arrays (MEA) in control conditions (DMSO, 2 hours) displayed spontaneous, low-frequency (<40Hz) events identified as interictal-like discharges (IILDs, **Fig. 5**). IILDs often originated from only a small subregion of the slice, usually in the subiculum or the dentate gyrus (**Table 1**, **Fig. 5, A** to **B**). In tissue preincubated with DMSO alone, IILDs had a mean amplitude of 57.3±13.5 µV and occurred at a mean frequency of 0.4±0.1 Hz. As observed previously *(7)*, the NKCC1 antagonist bumetanide (10 µM) partially reduced the amplitude and frequency of IILDs (**Fig. 5B**). However, these events were almost completely abolished in slices of the same resected tissue incubated for 2 hours with either 10 µM PCPZ (**Fig. 5B**) or 100 µM CLP-257 (**Fig. 5C**). Overall, both PCPZ and CLP-257 significantly reduced the proportion of slices displaying spontaneous

IILDs ($p<0.05$ for both; **Fig. 5D**). This effect did not reflect compromised neuronal activity, as IILD and multi-unit activity could be restored in slices pre-treated with PCPZ or CLP-257 by increasing neuronal excitability with high potassium, low magnesium ACSF (**Fig. 5, E** to **F**).

In slices from a group of 5 patients with mTLE (patients #5, 7, 8, 11, 12; group I; see **Table 1**), PCPZ virtually abolished IILDs (-97.6±13.8% change in frequency, $p<0.001$; **Fig. 5G**). In one slice of patient #3 and in the slices of patient #6 (group II), however, PCPZ failed to reduce the frequency of IILDs (+25.5±15.9%, $p=0.356$; **Fig. 5G**). Interestingly, neuropathological exploration of the resected tissue from patient #6 revealed an ILAE type 3 HS (**Table 1**), a rarer pattern of HS often associated with dual pathology *(50)*.

Similarly, preincubation with CLP-257 virtually abolished IILDs in slices from 5 out of 6 patients (-96.5±2.3% change in frequency, $p<0.001$; **Fig. 5G**). In slices from the remaining patient (#9, **Table 1**), however, CLP-257 failed to reduce the frequency of IILDs (+12.6%, **Fig. 5G**). Interestingly, again, neuropathological examination of this patient's postoperative tissue did not reveal hippocampal sclerosis, but rather a ganglioglioma associated with a somatic $BRAF^{V600E}$ mutation. Overall, these data demonstrate that enhancing KCC2 function prevents epileptiform activity recorded *in vitro* in postoperative tissue from a majority of patients with mTLE and typical ILAE type 1 HS.

PCPZ reduces interictal activity and seizures in a mouse model of mTLE

Spontaneous ictal activity is rarely observed in postoperative mTLE tissue slices *in vitro (48, 51)*. To assess the anti-seizure potential of KCC2 enhancers, we therefore tested their effect in a lithium-pilocarpine model of mTLE *(52)* adapted to mice (**Fig. 6A**). Since PCPZ but not CLP-

257 *(23)* can be readily used for chronic *in vivo* administration, we conducted these experiments with PCPZ. Status epilepticus (SE) was induced by intraperitoneal injection of the muscarinic agonist pilocarpine (see Supplementary Material and Methods). Mice typically developed SE within 10 to 20 minutes after pilocarpine injection and SE was interrupted after 1 hour by i.p. injection of diazepam and ketamine. Telemetric ECoG recordings revealed intense interictal discharge (IID) activity and occasional seizures for hours to a few days after SE, followed by a seizure-free, latent period that lasted 3 to 4 weeks before regular, spontaneous seizures were detected (**Fig. 6B, E**). Typical epileptiform activity such as interictal discharges (<20 Hz) or high-frequency oscillations (>80 Hz, HFOs, *(53–55)*) were also observed (**Fig. 6G** to **H**). In addition to these electrophysiological biomarkers, typical histological landmarks were detected in the hippocampus of these mice, including hippocampal sclerosis, granule cell dispersion, mossy fiber sprouting, and reduced KCC2 immunoreactivity in the dentate gyrus (**Fig. 6C** to **D**). After a 5-day habituation period with twice-daily saline injections (days 35-39, control period), we tested the effect of saline vs. PCPZ (2 mg/kg, i.p., 9AM and 8PM) on the occurrence of seizures and epileptiform events (IIDs, HFOs) during the next 5 days (days 40-44 post-SE, test period) (**Fig. 6A, E**).

Whereas seizure frequency was not significantly affected in animals receiving saline during the test period (0.15±0.07 vs. 0.18±0.06 seizures/hour, n=8 animals, p=0.118), animals receiving PCPZ showed an approximately 40% reduction in seizure frequency compared with the control period (0.09±0.05 vs. 0.14±0.05 seizures/hour, p=0.01; **Fig. 6F**). However, PCPZ had no effect on seizure duration (29.8±1.8 vs. 31.3±3.8 s, p=0.657) or power (7422±2736 vs. 6695±2058 mV^2, p=0.466; **Fig. 6F**), suggesting that it may be acting on mechanisms involved in seizure

onset rather than maintenance. In addition, and in agreement with our *in vitro* results on postoperative human tissue, PCPZ significantly reduced the frequency of IIDs by about 34% compared with control (192.0±39.3 vs. 290.9±60.3 IID/hour, p=0.01; **Fig. 6G**). The effect of PCPZ was even stronger on the frequency of HFOs, with a 58% reduction in mice receiving PCPZ (54.61±23.73 vs. 128.68±71.88 HFO/hour p=0.012), whereas HFO frequency increased by 38% in the saline only group (102.5±36.6 vs. 64.7±23.7 HFO/hour, p=0.027; **Fig. 6H**). Interestingly, although we observed a circadian rhythmicity in the occurrence of seizures and interictal activity (Fig. S6), as previously reported *(56, 57)*, the effect of PCPZ was similar during light (Zeitgeber time 0-12 h) and dark (Zeitgeber time 12-24 h) phases. These data demonstrate that PCPZ reduces chronic seizures and epileptiform activities (including HFOs and IIDs) in an animal model of mTLE.

Discussion

In this study we evaluated the effect and mode of action of two candidate KCC2 enhancers, PCPZ and CLP-257, in hippocampal neurons. Both reduce the lateral diffusion of KCC2, and increase its clustering and transport function. This effect is independent of changes in KCC2 expression and the phosphorylation level of its canonical residues and the WNK/SPAK pathway. In addition to this effect on KCC2 function, we also showed that CLP-257 directly modulates extrasynaptic but not synaptic $GABA_A$Rs. Furthermore, both compounds suppressed spontaneous, interictal-like discharges recorded in postoperative hippocampal tissue resected from patients with refractory mTLE. Finally, chronic administration of PCPZ reduced the occurrence of seizures and the frequency of interictal events in a mouse model of mTLE. Thus, our results provide a proof-of-concept of the therapeutic potential of KCC2 enhancers in a drug-resistant form of epilepsy and suggest that these compounds may also have therapeutic potential in other pathologies involving decreased KCC2 expression.

Several forms of epilepsy are associated with chloride transport dysfunction *(58)*, leading to paradoxically excitatory signaling by $GABA_A$ receptors *(7, 10)*. Although pro-GABAergic drugs such as benzodiazepines and other $GABA_A$ receptor positive allosteric modulators are often effective in epilepsy *(59)*, acting to directly potentiate GABA signaling when intraneuronal chloride levels are abnormal may fail to prevent seizures. Restoration of neuronal transmembrane chloride gradients therefore appears to be a promising first-line therapeutic strategy in drug-resistant epilepsy. In principle, this may be achieved by blocking chloride import, using NKCC1 antagonists such as bumetanide. Although this approach has been successfully used in some animal models of CNS disorders *(60–63)* it is not optimal as i)

bumetanide is largely bound to plasma proteins and very poorly crosses the blood brain barrier, ii) undergoes active efflux transport from the brain by organic anion transporters *(64, 65)* and iii) NKCC1 is widely expressed in many peripheral organs and tissues *(66)*, raising issues regarding the number of undesirable side effects. Instead, KCC2 is almost exclusively expressed in neurons, making it a prime target for neurological disorders associated with deficits in neuronal chloride homeostasis, such as mTLE. Acting to promote KCC2 function, even when its expression may be reduced in the pathology, may then help rescuing neuronal transmembrane chloride gradients and inhibitory GABA signaling.

CL-058 was the first compound identified as a candidate KCC2 enhancer by a small molecule library screening in a rodent neuroblastoma-glioma hybrid cell line *(23)*. It was then chemically optimized into CLP-257 and CLP-290, with improved EC50 and half-life for *in vivo* applications. While CLP drugs were initially described as specific KCC2 enhancers with little or no activity on other cation-chloride cotransporters *(23)*, a more recent study challenged this view and showed no effect on KCC2 function *(29)*. Instead, this study found direct binding and potentiating action on $GABA_A$ receptors. Although still controversial *(30)*, these results have called into question CLP drugs as pure KCC2 enhancing molecules. Our results now demonstrate that CLP-257 acts both as a *bona fide* KCC2 enhancer (Fig. 1) and a positive allosteric modulator of extrasynaptic, but not synaptic, $GABA_A$ receptors (Fig. 2) in rat hippocampal neurons. These data thus reconcile apparently conflicting results obtained on tonic $GABA_A$ receptor-mediated currents in hippocampal neurons *(29)* and mIPSCs from spinal cord neurons *(30)*. PCPZ on the other hand is a first-generation antipsychotic and is generally known as a dopamine D2 antagonist, although it interacts with a lower affinity with serotoninergic,

adrenergic, muscarinic and histaminergic receptors *(67–69)*. It was first suggested as a candidate KCC2 enhancer by screening Prestwick's library on HEK cells expressing recombinant KCC2 *(24)*, and was shown to reduce the depolarizing driving force of evoked IPSCs in immature rat spinal motoneurons after spinal cord injury. However, its effects on cortical neurons have not been investigated. Our results now show that PCPZ also acts as an effective KCC2 enhancer, increasing KCC2 function with no detectable effect on NKCC1. In contrast to CLP-257, however, PCPZ did not affect either phasic or tonic $GABA_A$ receptor-mediated IPSCs (Fig. 2).

Despite their potential therapeutic interest in rescuing chloride transport function in the pathology, the mechanisms of action of CLP-257 and PCPZ on KCC2 have not been fully characterized. Several studies have reported an increased total *(27, 28)* or plasmalemmal *(23, 26, 70)* KCC2 expression by CLP compounds, mostly in animal models of chronic pain or spasticity. Similarly, PCPZ was shown to rescue KCC2 membrane immunoreactivity in lumbar motoneurons after spinal cord injury *(24)*. However, the underlying mechanisms of these effects were not further investigated. We did not observe such changes in KCC2 expression upon incubation with PCPZ or CLP-257 in hippocampal neurons. Thus, both biochemical and immunofluorescence assays revealed no change in either total or plasmalemmal KCC2 expression levels (Fig. 3 and 4). Instead, increased KCC2 function was associated with reduced membrane lateral diffusion and increased clustering of KCC2 (Fig. 4). These observations suggest that, at least under non-pathological conditions, PCPZ and CLP-257 may primarily induce a redistribution of the membrane pool of KCC2 rather than a change in expression levels.

Previous studies have revealed that KCC2 lateral diffusion and clustering in the plasma membrane are tightly correlated with function and are controlled by phosphorylation of key

residues in its carboxy-terminal domain *(11, 39, 40, 71)*, making them prime candidate targets for KCC2 modulators. In particular, phosphorylation of serine 940 and dephosphorylation of threonines 906 and 1007 promote KCC2 clustering and membrane stability *(37, 40, 45, 47, 72)*. This effect usually results in increased membrane expression of the transporter, which was not observed upon PCPZ or CLP-257 treatment, making it unlikely that a modification of their phosphorylation underlies the effect of these compounds. Consistent with this conclusion, CLP-257 and PCPZ produced no significant change in the phosphorylation of these residues (Fig. 4) and did not affect the WNK/SPAK/OSR1 pathway known to phosphorylate T906 and T1007 *(37, 72)*. These observations are also consistent with the lack of effect of CLP290 on the phosphorylation of these residues in a mouse model of ischemia *(28)*. Finally, phosphorylation of tyrosine 1087 has been suggested to specifically impact KCC2 membrane clustering and function without affecting its membrane expression level *(47, 73, 74)* and would therefore be a good candidate target for PCPZ and CLP-257. However, KCC2 tyrosine phosphorylation was also unaffected in hippocampo-cortical slices upon PCPZ or CLP-257 treatment. Further investigation will be needed to test whether compensatory phosphorylation and dephosphorylation of distinct tyrosine residues may mask the net effect of KCC2 enhancers on Y1087.

Taken together, our data demonstrate for the first time that both PCPZ and CLP-257 enhance KCC2 function and promote its membrane confinement and clustering independent of apparent changes in the phosphorylation state of its canonical regulatory sites. Interestingly, a recent study has shown that other KCC2 enhancers with unknown mode of action display the same potentiating effect without affecting KCC2 membrane expression or the phosphorylation of S940

or T1007 residues *(75)*. PCPZ, CLP-257 and probably other KCC2 enhancers may act on alternative phosphorylation sites, as identified in large-scale proteomics studies *(75–77)*. Alternatively, they may interfere with KCC2 molecular interactions, without necessarily binding directly to KCC2. Thus, functional proteomics studies *(41, 76, 78)* have shown that KCC2 interacts with a variety of protein partners, some of which regulate its membrane expression and clustering. In particular, KCC2 interaction with the SNARE proteins SNAP23 and syntaxin 1A is essential for mZnR/GPR39-dependent upregulation of KCC2 activity *(79)*. Other candidates such as CIP1 *(80)*, Neto2 *(81)*, CKB *(82)*, PAM *(83)* and gephyrin *(41)* are of particular interest since their interaction with KCC2 was shown to increase its function. Finally, KCC2 enhancers may act to promote KCC2 accumulation into lipid rafts *(42)*, resulting in enhanced transporter membrane clustering and function.

Although some studies have reported effects of KCC2 enhancers on epileptiform activity *in vitro* or acute seizures such as *status epilepticus* in animal models, our work is the first to evaluate the therapeutic potential of KCC2 enhancers in the context of mTLE. Thus, CLP-257 was shown to either increase *(31)* or decrease *(32)* ictal-like discharges (ILDs) in two *in vitro* models of epileptiform activity. On the other hand, inhibition of the WNK/SPAK/OSR1 pathway with the WNK inhibitor WNK463 prevented KCC2 T1007 phosphorylation and reduced the intensity of kainate-induced *status epilepticus* in mice *(84)*. However, it remains to be determined whether this effect is strictly dependent on KCC2 potentiation or other effects of WNK inhibition, including on the NKCC1 transporter *(84)*. Finally, CLP290 was shown to reduce the sensitivity to pentylenetetrazole-induced seizures in a neonatal ischemic mouse model *(28)* while other KCC2 enhancers prevented the development of and terminated kainate-induced *status epilepticus*

(75). Unfortunately, this study did not investigate the effect of KCC2 enhancers on spontaneous and recurrent seizures that characterize mTLE.

Our new data now demonstrate that both PCPZ and CLP-257 increase KCC2 function and suppress spontaneous epileptiform activity recorded *in vitro* from human postoperative tissue from mTLE patients as well as interictal activity and seizures in a mouse model of mTLE. It is noteworthy that out of 13 temporal lobe resective tissues, PCPZ or CLP-257 near-completely suppressed interictal-like activity in 10 samples, whereas it had virtually no effect in 3 of them (Fig. 5). Neuropathological analysis of these patients revealed that they had rare forms of temporal lobe epilepsy, one related to a ganglioglioma associated with a somatic mutation of the BRAF proto-oncogene, and the other of ILAE type 3, often associated with a dual pathology. Further investigation of the phenotype of these non-responding tissues will be necessary to elucidate their pathophysiological characteristics and the origin of their resistance to KCC2 enhancers.

PCPZ is a first-generation antipsychotic with FDA approval and indications in schizophrenia, migraine as well as nausea and vomiting *(85)*. Side effects are generally mild in adults but adverse effects such as sedation, extrapyramidal symptoms, and in some rare cases, seizures, have been reported in children *(86)*. Instead, we now provide evidence that PCPZ shows significant antiepileptic properties both in postoperative temporal lobe tissue from mTLE patients *in vitro*, and in a mouse model of mTLE. *In vitro*, the effect of PCPZ was at least comparable to that of bumetanide as described in postoperative epileptic brain tissue from patients with epilepsy of various etiology *(5, 7, 10)*, adding to the evidence that rescuing neuronal chloride transport may be an effective anti-epileptic strategy. *In vivo*, PCPZ reduced

seizure occurrence by about two-fold (Fig. 6) but also strongly reduced interictal discharges and high-frequency oscillations, two hallmarks of epileptic networks *(53–55)*. *In vivo*, PCPZ was used at a concentration of 2 mg/kg through i.p. injections. At this dosage in mice, PCPZ likely acts mainly on D2 dopamine receptors, but without any side effect on motility, exploratory behavior or motor coordination of the animals *(87)*. It seems unlikely that the antiseizure effect of PCPZ *in vivo* may be mediated by D2 receptor antagonism since reduced D2 receptor expression or function is associated with increased, not decreased, seizure threshold *(88)*. In addition, D2 agonists, not antagonists, were shown to display antiepileptic properties *(88)*. Altogether, our results demonstrate that PCPZ, like CLP-257, is an effective KCC2 enhancer and that KCC2 activation may be an effective strategy in mTLE in patients. The recent progress in elucidating the molecular structure of KCC2 *(89–92)* provides a unique opportunity to explore the molecular mechanisms underlying the modulation of its expression and function and design more specific, structure-based KCC2 enhancers with improved efficacy and specificity.

Material and Methods

Study Design

The purpose of this study was to identify the effect and mode of action of two candidate KCC2 enhancers (CLP-257 and PCPZ) and to test their antiepileptic potential in mTLE. First, the effect of these compounds on KCC2 and $GABA_AR$ function was investigated by performing *in vitro* electrophysiology on rat hippocampal neurons. Secondly, the effect of CLP-257 and PCPZ on KCC2 expression, diffusion and clustering was explored by combining biochemistry, single particle tracking and immunocytochemistry experiments respectively, in rat hippocampal neurons. Subsequently, changes in phosphorylation of canonical KCC2 regulatory residues after treatment with these KCC2 enhancers were addressed by performing immunoprecipitation assays in hippocampo-cortical slices from adult rats. Finally, the antiepileptic potential of these compounds was investigated *in vitro* by performing multi-electrode array recordings on postoperative tissue from mTLE patients and *in vivo* by conducting ECoG recordings in a mouse model of mTLE.

The indicated number of observations corresponds to the number of cells for electrophysiology and immunocytochemistry data, individual quantum dots for single particle tracking, independent primary hippocampal cultures or animals for biochemistry, animals for *in vivo* experiments, and slices or patients for human tissue recordings. Sample size selection for experiments was based on published experiments, pilot studies, as well as in-house expertise.

Most of the experiment's analyses were blinded to the treatment conditions. In addition, semi-automated analysis software was used to reduce human bias. Human hippocampal slices were

randomly assigned to either the control or treatment paradigm prior to conducting the experiments. Finally, animals were randomly assigned to treatment groups with approximately equal numbers in each condition.

Animal experimentation

All animal procedures were carried out according to the European Community Council directive of 24 November 1986 (86/609/EEC) and the guidelines of the French Agriculture and Forestry Ministry for handling animals (decree 87-848), and were approved by the "Direction Départementale de la Protection des Populations de Paris" (authorization number D75-05-22). Procedures had been assessed by the site's animal welfare structure and the local ethics committee n°5 (Charles Darwin). Following the favorable opinion of the ethics committee of our project APAFIS#24889-202008050923999 v4, we obtained the authorization from the Ministry of Research and Higher Education to carry out the experiments on animals used for scientific purposes.

Patients

Informed consent to participate in the study was obtained from patients or their legal guardians. The protocol received a favorable opinion of a research ethics committee (CPP Île-de-France 1 - 14388, January 16, 2017). A small part of non-essential brain tissue for neuropathological diagnostic purposes was attributed to research by the neurosurgeon during surgery, in agreement with the neuropathologist and the neurologist. Brain samples were obtained between 2017 and 2021 from 13 patients (4 males, 9 females, age range: 16-63 years, Table 1) diagnosed with

mesial temporal lobe epilepsy that was associated with hippocampal sclerosis (11 patients), glioneuronal tumor (1 patient) and hippocampal atrophy with malformation of cortical development (polymicrogyria and subcortical heterotopia, 1 patient). Patients underwent multimodal preoperative work-up including neurological, neuropsychological assessment video-electroencephalographic recording, magnetic resonance imaging and fluorodeoxyglucose positron emission tomography. In addition, stereoelectroencephalography was performed in 6 patients.

Corticectomies were performed at Sainte-Anne Hospital (9 patients) and at Pitié-Salpêtrière Hospital (4 patients) Neuropathological diagnosis was made according to the classification of the Diagnostic Methods Commission of the International League Against Epilepsy (ILAE) (*50).*

Statistical Analysis

Means are shown ± SEM, median values are indicated with their interquartile range (IQR, 25–75%). Means were compared using Student's parametric t-test when statistical conditions were verified (normal distribution and homoscedasticity). Otherwise, a non-parametric Mann-Whitney (MW) test was performed. For paired measurements, Wilcoxon test were used unless statistical conditions were verified for Student’s paired t-test. Statistical tests were performed using SigmaPlot 13 (Systat Software). Differences were considered significant for p-values less than 5 % (* $p \leq 0.05$, ** $p < 0.01$, *** $p < 0.001$). Error bars correspond to SEM.

List of Supplementary Materials:

Material and Methods

Fig. S1. PCPZ and CLP-257 do not affect membrane or series resistance.

Fig. S2. CLP-257 modulates $GABA_A$ receptor function at micromolar concentrations.

Fig. S3. PCPZ and CLP-257 do not affect NKCC1 total or plasmalemmal expression levels.

Fig. S4. The D2R antagonist eticlopride does not affect KCC2 clustering in hippocampal neurons.

Fig. S5. PCPZ and CLP-257 do not inhibit kinase activity of the WNK/SPAK/OSR1 pathway.

Fig. S6. PCPZ reduces seizure frequency and interictal activity independent of their circadian modulation.

References

1. A. K. Ngugi, C. Bottomley, I. Kleinschmidt, J. W. Sander, C. R. Newton, Estimation of the burden of active and life-time epilepsy: A meta-analytic approach. *Epilepsia* **51**, 883–890 (2010).

2. I. Blumcke, R. Spreafico, G. Haaker, R. Coras, K. Kobow, C. G. Bien, M. Pfäfflin, C. Elger, G. Widman, J. Schramm, A. Becker, K. P. Braun, F. Leijten, J. C. Baayen, E. Aronica, F. Chassoux, H. Hamer, H. Stefan, K. Rössler, M. Thom, M. C. Walker, S. M. Sisodiya, J. S. Duncan, A. W. McEvoy, T. Pieper, H. Holthausen, M. Kudernatsch, H. J. Meencke, P. Kahane, A. Schulze-Bonhage, J. Zentner, D. H. Heiland, H. Urbach, B. J. Steinhoff, T. Bast, L. Tassi, G. Lo Russo, C. Özkara, B. Oz, P. Krsek, S. Vogelgesang, U. Runge, H. Lerche, Y. Weber, M. Honavar, J. Pimentel, A. Arzimanoglou, A. Ulate-Campos, S. Noachtar, E. Hartl, O. Schijns, R. Guerrini, C. Barba, T. S. Jacques, J. H. Cross, M. Feucht, A. Mühlebner, T. Grunwald, E. Trinka, P. A. Winkler, A. Gil-Nagel, R. Toledano Delgado, T. Mayer, M. Lutz, B. Zountsas, K. Garganis, F. Rosenow, A. Hermsen, T. J. von Oertzen, T. L. Diepgen, G. Avanzini, Histopathological Findings in Brain Tissue Obtained during Epilepsy Surgery. *New England Journal of Medicine* **377**, 1648–1656 (2017).

3. A. J. Lowe, E. David, C. J. Kilpatrick, Z. Matkovic, M. J. Cook, A. Kaye, T. J. O'Brien, Epilepsy Surgery for Pathologically Proven Hippocampal Sclerosis Provides Long-term Seizure Control and Improved Quality of Life. *Epilepsia* **45**, 237–242 (2004).

4. J. de Tisi, G. S. Bell, J. L. Peacock, A. W. McEvoy, W. F. J. Harkness, J. W. Sander, J. S. Duncan, The long-term outcome of adult epilepsy surgery, patterns of seizure remission, and relapse: a cohort study. *Lancet* **378**, 1388–1395 (2011).

5. T. Blauwblomme, E. Dossi, C. Pellegrino, E. Goubert, B. G. Iglesias, C. Sainte-Rose, N. Rouach, R. Nabbout, G. Huberfeld, Gamma-aminobutyric acidergic transmission underlies interictal epileptogenicity in pediatric focal cortical dysplasia. *Annals of Neurology* **85**, 204–217 (2019).

6. I. Cohen, V. Navarro, S. Clemenceau, M. Baulac, R. Miles, On the Origin of Interictal Activity in Human Temporal Lobe Epilepsy in Vitro. *Science* **298**, 1418–1421 (2002).

7. G. Huberfeld, L. Wittner, S. Clemenceau, M. Baulac, K. Kaila, R. Miles, C. Rivera, Perturbed Chloride Homeostasis and GABAergic Signaling in Human Temporal Lobe Epilepsy. *J. Neurosci.* **27**, 9866–9873 (2007).

8. M. Munakata, M. Watanabe, T. Otsuki, H. Nakama, K. Arima, M. Itoh, J. Nabekura, K. Iinuma, S. Tsuchiya, Altered distribution of KCC2 in cortical dysplasia in patients with intractable epilepsy. *Epilepsia* **48**, 837–844 (2007).

9. A. Muñoz, P. Méndez, J. DeFelipe, F. J. Alvarez-Leefmans, Cation-Chloride Cotransporters and GABA-ergic Innervation in the Human Epileptic Hippocampus. *Epilepsia* **48**, 663–673 (2007).

10. J. Pallud, M. Le Van Quyen, F. Bielle, C. Pellegrino, P. Varlet, N. Cresto, M. Baulac, C. Duyckaerts, N. Kourdougli, G. Chazal, B. Devaux, C. Rivera, R. Miles, L. Capelle, G.

Huberfeld, Cortical GABAergic excitation contributes to epileptic activities around human glioma. *Sci Transl Med* **6**, 244ra89-244ra89 (2014).

11. P. Blaesse, M. S. Airaksinen, C. Rivera, K. Kaila, Cation-Chloride Cotransporters and Neuronal Function. *Neuron* **61**, 820–838 (2009).

12. H. R. Pathak, F. Weissinger, M. Terunuma, G. C. Carlson, F.-C. Hsu, S. J. Moss, D. A. Coulter, Disrupted Dentate Granule Cell Chloride Regulation Enhances Synaptic Excitability during Development of Temporal Lobe Epilepsy. *J Neurosci* **27**, 14012–14022 (2007).

13. M. R. Karlócai, L. Wittner, K. Tóth, Z. Maglóczky, Z. Katarova, G. Rásonyi, L. Erőss, S. Czirják, P. Halász, G. Szabó, J. A. Payne, K. Kaila, T. F. Freund, Enhanced expression of potassium-chloride cotransporter KCC2 in human temporal lobe epilepsy. *Brain Struct Funct* **221**, 3601–3615 (2016).

14. M. Goutierre, S. A. Awabdh, F. Donneger, E. François, D. Gomez-Dominguez, T. Irinopoulou, L. M. de la Prida, J. C. Poncer, KCC2 Regulates Neuronal Excitability and Hippocampal Activity via Interaction with Task-3 Channels. *Cell Reports* **28**, 91-103.e7 (2019).

15. M. R. Kelley, R. A. Cardarelli, J. L. Smalley, T. A. Ollerhead, P. M. Andrew, N. J. Brandon, T. Z. Deeb, S. J. Moss, Locally Reducing KCC2 Activity in the Hippocampus is Sufficient to Induce Temporal Lobe Epilepsy. *EBioMedicine* **32**, 62–71 (2018).

16. G. Di Cristo, P. N. Awad, S. Hamidi, M. Avoli, KCC2, epileptiform synchronization, and epileptic disorders. *Progress in Neurobiology* **162**, 1–16 (2018).

17. T. J. Ellender, J. V. Raimondo, A. Irkle, K. P. Lamsa, C. J. Akerman, Excitatory Effects of Parvalbumin-Expressing Interneurons Maintain Hippocampal Epileptiform Activity via Synchronous Afterdischarges. *J Neurosci* **34**, 15208–15222 (2014).

18. R. Khazipov, G. Valeeva, I. Khalilov, Depolarizing GABA and Developmental Epilepsies. *CNS Neurosci Ther* **21**, 83–91 (2014).

19. Y. E. Moore, T. Z. Deeb, H. Chadchankar, N. J. Brandon, S. J. Moss, Potentiating KCC2 activity is sufficient to limit the onset and severity of seizures. *Proceedings of the National Academy of Sciences* **115**, 10166–10171 (2018).

20. V. Magloire, J. Cornford, A. Lieb, D. M. Kullmann, I. Pavlov, KCC2 overexpression prevents the paradoxical seizure-promoting action of somatic inhibition. *Nat Commun* **10**, 1225–1237 (2019).

21. R. M. Pressler, G. B. Boylan, N. Marlow, M. Blennow, C. Chiron, J. H. Cross, L. S. de Vries, B. Hallberg, L. Hellström-Westas, V. Jullien, V. Livingstone, B. Mangum, B. Murphy, D. Murray, G. Pons, J. Rennie, R. Swarte, M. C. Toet, S. Vanhatalo, S. Zohar, Bumetanide for the treatment of seizures in newborn babies with hypoxic ischaemic encephalopathy (NEMO): an open-label, dose finding, and feasibility phase 1/2 trial. *The Lancet Neurology* **14**, 469–477 (2015).

22. J. S. Soul, A. M. Bergin, C. Stopp, B. Hayes, A. Singh, C. R. Fortuno, D. O'Reilly, K. Krishnamoorthy, F. E. Jensen, V. Rofeberg, M. Dong, A. A. Vinks, D. Wypij, K. J. Staley, A

Pilot Randomized, Controlled, Double-Blind Trial of Bumetanide to Treat Neonatal Seizures. *Ann Neurol* **89**, 327–340 (2021).

23. M. Gagnon, M. J. Bergeron, G. Lavertu, A. Castonguay, S. Tripathy, R. P. Bonin, J. Perez-Sanchez, D. Boudreau, B. Wang, L. Dumas, I. Valade, K. Bachand, M. Jacob-Wagner, C. Tardif, I. Kianicka, P. Isenring, G. Attardo, J. A. M. Coull, Y. De Koninck, Chloride extrusion enhancers as novel therapeutics for neurological diseases. *Nat Med* **19**, 1524–1528 (2013).

24. S. Liabeuf, L. Stuhl-Gourmand, F. Gackière, R. Mancuso, I. Sanchez Brualla, P. Marino, F. Brocard, L. Vinay, Prochlorperazine Increases KCC2 Function and Reduces Spasticity after Spinal Cord Injury. *J Neurotrauma* **34**, 3397–3406 (2017).

25. A. J. Barbour, K. F. Hauser, A. R. McQuiston, P. E. Knapp, HIV and opiates dysregulate K+-Cl− cotransporter 2 (KCC2) to cause GABAergic dysfunction in primary human neurons and Tat-transgenic mice. *Neurobiol Dis* **141**, 104878 (2020).

26. J. Bilchak, K. Yeakle, G. Caron, D. Malloy, M.-P. Côté, Enhancing KCC2 activity decreases hyperreflexia and spasticity after chronic spinal cord injury. *Exp Neurol* **338**, 113605 (2021).

27. Y. Gao, W. Zhan, Y. Jin, X. Chen, J. Cai, X. Zhou, X. Huang, Q. Zhao, W. Wang, J. Sun, KCC2 receptor upregulation potentiates antinociceptive effect of GABAAR agonist on remifentanil-induced hyperalgesia. *Mol Pain* **18**, 17448069221082880 (2022).

28. B. J. Sullivan, P. A. Kipnis, B. M. Carter, L.-R. Shao, S. D. Kadam, Targeting ischemia-induced KCC2 hypofunction rescues refractory neonatal seizures and mitigates epileptogenesis in a mouse model. *Sci Signal* **14**, eabg2648 (2021).

29. R. A. Cardarelli, K. Jones, L. I. Pisella, H. J. Wobst, L. J. McWilliams, P. M. Sharpe, M. P. Burnham, D. J. Baker, I. Chudotvorova, J. Guyot, L. Silayeva, D. H. Morrow, N. Dekker, S. Zicha, P. A. Davies, J. Holenz, M. E. Duggan, J. Dunlop, R. J. Mather, Q. Wang, I. Medina, N. J. Brandon, T. Z. Deeb, S. J. Moss, The small molecule CLP257 does not modify activity of the K+–Cl− co-transporter KCC2 but does potentiate GABAA receptor activity. *Nat Med* **23**, 1394–1396 (2017).

30. M. Gagnon, M. J. Bergeron, J. Perez-Sanchez, I. Plasencia-Fernández, L.-E. Lorenzo, A. G. Godin, A. Castonguay, R. P. Bonin, Y. De Koninck, Reply to The small molecule CLP257 does not modify activity of the K+-Cl- co-transporter KCC2 but does potentiate GABAA receptor activity. *Nat Med* **23**, 1396–1398 (2017).

31. S. Hamidi, M. Avoli, KCC2 function modulates in vitro ictogenesis. *Neurobiol Dis* **79**, 51–58 (2015).

32. V. I. Dzhala, K. J. Staley, KCC2 Chloride Transport Contributes to the Termination of Ictal Epileptiform Activity. *eNeuro* **8**, ENEURO.0208-20.2020 (2021).

33. G. Gauvain, I. Chamma, Q. Chevy, C. Cabezas, T. Irinopoulou, N. Bodrug, M. Carnaud, S. Lévi, J. C. Poncer, The neuronal K-Cl cotransporter KCC2 influences postsynaptic AMPA receptor content and lateral diffusion in dendritic spines. *Proc Natl Acad Sci U S A* **108**, 15474–15479 (2011).

34. Y. Otsu, F. Donneger, E. J. Schwartz, J. C. Poncer, Cation–chloride cotransporters and the polarity of GABA signalling in mouse hippocampal parvalbumin interneurons. *The Journal of Physiology* **598**, 1865–1880 (2020).

35. S. Khirug, J. Yamada, R. Afzalov, J. Voipio, L. Khiroug, K. Kaila, GABAergic Depolarization of the Axon Initial Segment in Cortical Principal Neurons Is Caused by the Na–K–2Cl Cotransporter NKCC1. *J Neurosci* **28**, 4635–4639 (2008).

36. M. Chen, J. Wang, J. Jiang, X. Zheng, N. J. Justice, K. Wang, X. Ran, Y. Li, Q. Huo, J. Zhang, H. Li, N. Lu, Y. Wang, H. Zheng, C. Long, L. Yang, E. Kim, Ed. APP modulates KCC2 expression and function in hippocampal GABAergic inhibition. *eLife* **6**, e20142 (2017).

37. M. Heubl, J. Zhang, J. C. Pressey, S. Al Awabdh, M. Renner, F. Gomez-Castro, I. Moutkine, E. Eugène, M. Russeau, K. T. Kahle, J. C. Poncer, S. Lévi, GABAA receptor dependent synaptic inhibition rapidly tunes KCC2 activity via the Cl−-sensitive WNK1 kinase. *Nat Commun* **8**, 1776 (2017).

38. M. A. Virtanen, P. Uvarov, M. Mavrovic, J. C. Poncer, K. Kaila, The Multifaceted Roles of KCC2 in Cortical Development. *Trends in Neurosciences* **44**, 378–392 (2021).

39. E. Côme, M. Heubl, E. J. Schwartz, J. C. Poncer, S. Lévi, Reciprocal Regulation of KCC2 Trafficking and Synaptic Activity. *Frontiers in Cellular Neuroscience* **13,** 48 (2019)

40. I. Chamma, M. Heubl, Q. Chevy, M. Renner, I. Moutkine, E. Eugène, J. C. Poncer, S. Lévi, Activity-Dependent Regulation of the K/Cl Transporter KCC2 Membrane Diffusion, Clustering, and Function in Hippocampal Neurons. *J. Neurosci.* **33**, 15488–15503 (2013).

41. S. A. Awabdh, F. Donneger, M. Goutierre, M. Séveno, O. Vigy, P. Weinzettl, M. Russeau, I. Moutkine, S. Lévi, P. Marin, J. C. Poncer, Gephyrin Interacts with the K-Cl Cotransporter KCC2 to Regulate Its Surface Expression and Function in Cortical Neurons. *J. Neurosci.* **42**, 166–182 (2022).

42. M. Watanabe, H. Wake, A. J. Moorhouse, J. Nabekura, Clustering of Neuronal K+-Cl− Cotransporters in Lipid Rafts by Tyrosine Phosphorylation. *J Biol Chem* **284**, 27980–27988 (2009).

43. K. T. Kahle, A. R. Khanna, S. L. Alper, N. C. Adragna, P. K. Lauf, D. Sun, E. Delpire, K-Cl cotransporters, cell volume homeostasis, and neurological disease. *Trends Mol Med* **21**, 513–523 (2015).

44. H. H. C. Lee, T. Z. Deeb, J. A. Walker, P. A. Davies, S. J. Moss, NMDA receptor activity downregulates KCC2 resulting in depolarizing GABAA receptor mediated currents. *Nat Neurosci* **14**, 736–743 (2011).

45. P. delos Heros, D. R. Alessi, R. Gourlay, D. G. Campbell, M. Deak, T. J. Macartney, K. T. Kahle, J. Zhang, The WNK-regulated SPAK/OSR1 kinases directly phosphorylate and inhibit the K+–Cl− co-transporters. *Biochem J* **458**, 559–573 (2014).

46. K. Yamada, H.-M. Park, D. F. Rigel, K. DiPetrillo, E. J. Whalen, A. Anisowicz, M. Beil, J. Berstler, C. E. Brocklehurst, D. A. Burdick, S. L. Caplan, M. P. Capparelli, G. Chen, W. Chen, B. Dale, L. Deng, F. Fu, N. Hamamatsu, K. Harasaki, T. Herr, P. Hoffmann, Q.-Y. Hu, W.-J. Huang, N. Idamakanti, H. Imase, Y. Iwaki, M. Jain, J. Jeyaseelan, M. Kato, V. K. Kaushik, D.

Kohls, V. Kunjathoor, D. LaSala, J. Lee, J. Liu, Y. Luo, F. Ma, R. Mo, S. Mowbray, M. Mogi, F. Ossola, P. Pandey, S. J. Patel, S. Raghavan, B. Salem, Y. H. Shanado, G. M. Trakshel, G. Turner, H. Wakai, C. Wang, S. Weldon, J. B. Wielicki, X. Xie, L. Xu, Y. I. Yagi, K. Yasoshima, J. Yin, D. Yowe, J.-H. Zhang, G. Zheng, L. Monovich, Small-molecule WNK inhibition regulates cardiovascular and renal function. *Nat Chem Biol* **12**, 896–898 (2016).

47. H. H. C. Lee, R. Jurd, S. J. Moss, Tyrosine phosphorylation regulates the membrane trafficking of the potassium chloride co-transporter KCC2. *Mol Cell Neurosci* **45**, 173–179 (2010).

48. G. Huberfeld, L. Menendez de la Prida, J. Pallud, I. Cohen, M. Le Van Quyen, C. Adam, S. Clemenceau, M. Baulac, R. Miles, Glutamatergic pre-ictal discharges emerge at the transition to seizure in human epilepsy. *Nat Neurosci* **14**, 627–634 (2011).

49. C. Le Duigou, E. Savary, M. Morin-Brureau, D. Gomez-Dominguez, G. Milior, F. Chali, A. Sobczyk, E. Eugène, L. Kraus, J. C. Meier, D. M. Kullmann, B. Mathon, L. M. de la Prida, G. Dorfmuller, J. Pallud, S. Clemenceau, R. Miles, Imaging pathological activities of human brain tissue in organotypic culture. *J Neurosci Methods* **298**, 33–44 (2018).

50. I. Blümcke, M. Thom, E. Aronica, D. D. Armstrong, F. Bartolomei, A. Bernasconi, N. Bernasconi, C. G. Bien, F. Cendes, R. Coras, J. H. Cross, T. S. Jacques, P. Kahane, G. W. Mathern, H. Miyata, S. L. Moshé, B. Oz, Ç. Özkara, E. Perucca, S. Sisodiya, S. Wiebe, R. Spreafico, International consensus classification of hippocampal sclerosis in temporal lobe

epilepsy: A Task Force report from the ILAE Commission on Diagnostic Methods. *Epilepsia* **54**, 1315–1329 (2013).

51. G. Huberfeld, C. Le Duigou, M. Le Van Quyen, V. Navarro, M. Baulac, R. Miles, The Paradox of the Paroxysm: Can Seizure Precipitants Help Explain Human Ictogenesis? *Neuroscientist* **19**, 523–540 (2013).

52. G. Foffani, Y. G. Uzcategui, B. Gal, L. M. de la Prida, Reduced Spike-Timing Reliability Correlates with the Emergence of Fast Ripples in the Rat Epileptic Hippocampus. *Neuron* **55**, 930–941 (2007).

53. L. Menendez de la Prida, A. J. Trevelyan, Cellular mechanisms of high frequency oscillations in epilepsy: On the diverse sources of pathological activities. *Epilepsy Research* **97**, 308–317 (2011).

54. M. Zijlmans, P. Jiruska, R. Zelmann, F. S. S. Leijten, J. G. R. Jefferys, J. Gotman, High-Frequency Oscillations as a New Biomarker in Epilepsy. *Ann Neurol* **71**, 169–178 (2012).

55. M. Lévesque, P. Salami, Z. Shiri, M. Avoli, Interictal oscillations and focal epileptic disorders. *European Journal of Neuroscience* **48**, 2915–2927 (2018).

56. P. J. Karoly, V. R. Rao, N. M. Gregg, G. A. Worrell, C. Bernard, M. J. Cook, M. O. Baud, Cycles in epilepsy. *Nat Rev Neurol* **17**, 267–284 (2021).

57. M. Baud, A. Ghestem, J.-J. Benoliel, C. Becker, C. Bernard, Endogenous multidien rhythm of epilepsy in rats. *Experimental Neurology* **315**, 82 (2019).

58. R. J. Burman, R. E. Rosch, J. M. Wilmshurst, A. Sen, G. Ramantani, C. J. Akerman, J. V. Raimondo, Why won't it stop? The dynamics of benzodiazepine resistance in status epilepticus. *Nat Rev Neurol* **18**, 428–441 (2022).

59. L. J. Greenfield, Molecular Mechanisms of Antiseizure Drug Activity at GABAA Receptors. *Seizure* **22**, 589–600 (2013).

60. A. Banerjee, R. V. Rikhye, V. Breton-Provencher, X. Tang, C. Li, K. Li, C. A. Runyan, Z. Fu, R. Jaenisch, M. Sur, Jointly reduced inhibition and excitation underlies circuit-wide changes in cortical processing in Rett syndrome. *Proceedings of the National Academy of Sciences* **113**, E7287–E7296 (2016).

61. Z. Dargaei, J. Y. Bang, V. Mahadevan, C. S. Khademullah, S. Bedard, G. M. Parfitt, J. C. Kim, M. A. Woodin, Restoring GABAergic inhibition rescues memory deficits in a Huntington's disease mouse model. *Proc Natl Acad Sci U S A* **115**, E1618–E1626 (2018).

62. N. Kourdougli, C. Pellegrino, J.-M. Renko, S. Khirug, G. Chazal, T.-K. Kukko-Lukjanov, S. E. Lauri, J.-L. Gaiarsa, L. Zhou, A. Peret, E. Castrén, R. K. Tuominen, V. Crépel, C. Rivera, Depolarizing γ-aminobutyric acid contributes to glutamatergic network rewiring in epilepsy. *Annals of Neurology* **81**, 251–265 (2017).

63. N. Lozovaya, R. Nardou, R. Tyzio, M. Chiesa, A. Pons-Bennaceur, S. Eftekhari, T.-T. Bui, M. Billon-Grand, J. Rasero, P. Bonifazi, D. Guimond, J.-L. Gaiarsa, D. C. Ferrari, Y. Ben-Ari, Early alterations in a mouse model of Rett syndrome: the GABA developmental shift is abolished at birth. *Sci Rep* **9**, 9276 (2019).

64. W. Löscher, K. Kaila, CNS pharmacology of NKCC1 inhibitors. *Neuropharmacology* **205**, 108910 (2022).

65. A. Savardi, M. Borgogno, M. De Vivo, L. Cancedda, Pharmacological tools to target NKCC1 in brain disorders. *Trends Pharmacol Sci* **42**, 1009–1034 (2021).

66. E. Delpire, K. B. Gagnon, in *Comprehensive Physiology*, (John Wiley & Sons, Ltd, 2018), pp. 871–901.

67. J. S. Silvestre, J. Prous, Research on adverse drug events. I. Muscarinic M3 receptor binding affinity could predict the risk of antipsychotics to induce type 2 diabetes. *Methods Find Exp Clin Pharmacol* **27**, 289–304 (2005).

68. E. Richelson, A. Nelson, Antagonism by neuroleptics of neurotransmitter receptors of normal human brain in vitro. *Eur J Pharmacol* **103**, 197–204 (1984).

69. H. Appl, T. Holzammer, S. Dove, E. Haen, A. Strasser, R. Seifert, Interactions of recombinant human histamine H□R, H□R, H□R, and H□R receptors with 34 antidepressants and antipsychotics. *Naunyn Schmiedebergs Arch Pharmacol* **385**, 145–170 (2012).

70. F. Ferrini, L.-E. Lorenzo, A. G. Godin, M. L. Quang, Y. De Koninck, Enhancing KCC2 function counteracts morphine-induced hyperalgesia. *Sci Rep* **7**, 3870 (2017).

71. A.-M. Hartmann, H. G. Nothwang, NKCC1 and KCC2: Structural insights into phospho-regulation. *Front Mol Neurosci* **15**, 964488 (2022).

72. P. Friedel, K. T. Kahle, J. Zhang, N. Hertz, L. I. Pisella, E. Buhler, F. Schaller, J. Duan, A. R. Khanna, P. N. Bishop, K. M. Shokat, I. Medina, WNK1-regulated inhibitory phosphorylation of the KCC2 cotransporter maintains the depolarizing action of GABA in immature neurons. *Sci Signal* **8**, ra65 (2015).

73. K. Strange, T. D. Singer, R. Morrison, E. Delpire, Dependence of KCC2 K-Cl cotransporter activity on a conserved carboxy terminus tyrosine residue. *American Journal of Physiology-Cell Physiology* **279**, C860–C867 (2000).

74. M. Wantanabe, J. Zhang, M. S. Mansuri, J. Duan, J. K. Karimy, E. Delpire, S. L. Alper, R. P. Lifton, A. Fukuda, K. T. Kahle, Developmentally regulated KCC2 phosphorylation is essential for dynamic GABA-mediated inhibition and survival. *Sci Signal* **12**, eaaw9315 (2019).

75. R. Jarvis, S. F. Josephine Ng, A. J. Nathanson, R. A. Cardarelli, K. Abiraman, F. Wade, A. Evans-Strong, M. P. Fernandez-Campa, T. Z. Deeb, J. L. Smalley, T. Jamier, I. K. Gurrell, L. McWilliams, A. Kawatkar, L. C. Conway, Q. Wang, R. W. Burli, N. J. Brandon, I. P. Chessell, A. J. Goldman, J. L. Maguire, S. J. Moss, Direct activation of KCC2 arrests benzodiazepine refractory status epilepticus and limits the subsequent neuronal injury in mice. *Cell Rep Med* **4**, 100957 (2023).

76. A. Cordshagen, W. Busch, M. Winklhofer, H. G. Nothwang, A.-M. Hartmann, Phosphoregulation of the intracellular termini of K+-Cl− cotransporter 2 (KCC2) enables flexible control of its activity. *J Biol Chem* **293**, 16984–16993 (2018).

77. J. L. Smalley, G. Kontou, C. Choi, Q. Ren, D. Albrecht, K. Abiraman, M. A. R. Santos, C. E. Bope, T. Z. Deeb, P. A. Davies, N. J. Brandon, S. J. Moss, Isolation and Characterization of Multi-Protein Complexes Enriched in the K-Cl Co-transporter 2 From Brain Plasma Membranes. *Frontiers in Molecular Neuroscience* **13**, 563091 (2020).

78. M. Weber, A.-M. Hartmann, T. Beyer, A. Ripperger, H. G. Nothwang, A Novel Regulatory Locus of Phosphorylation in the C Terminus of the Potassium Chloride Cotransporter KCC2 That Interferes with N-Ethylmaleimide or Staurosporine-mediated Activation. *J Biol Chem* **289**, 18668–18679 (2014).

79. V. Mahadevan, C. S. Khademullah, Z. Dargaei, J. Chevrier, P. Uvarov, J. Kwan, R. D. Bagshaw, T. Pawson, A. Emili, Y. De Koninck, V. Anggono, M. Airaksinen, M. A. Woodin, M. B. Kennedy, Ed. Native KCC2 interactome reveals PACSIN1 as a critical regulator of synaptic inhibition. *eLife* **6**, e28270 (2017).

80. H. Asraf, M. Bogdanovic, N. Gottesman, I. Sekler, E. Aizenman, M. Hershfinkel, SNAP23 regulates KCC2 membrane insertion and activity following mZnR/GPR39 activation in hippocampalneurons. *iScience* **25**, 103751 (2022).

81. M. Wenz, A.-M. Hartmann, E. Friauf, H. G. Nothwang, CIP1 is an activator of the K+-Cl- cotransporter KCC2. *Biochem Biophys Res Commun* **381**, 388–392 (2009).

82. E. A. Ivakine, B. A. Acton, V. Mahadevan, J. Ormond, M. Tang, J. C. Pressey, M. Y. Huang, D. Ng, E. Delpire, M. W. Salter, M. A. Woodin, R. R. McInnes, Neto2 is a KCC2 interacting

protein required for neuronal Cl− regulation in hippocampal neurons. *Proceedings of the National Academy of Sciences* **110**, 3561–3566 (2013).

83. K. Inoue, J. Yamada, S. Ueno, A. Fukuda, Brain-type creatine kinase activates neuron-specific K+-Cl- co-transporter KCC2. *J Neurochem* **96**, 598–608 (2006).

84. N. Garbarini, E. Delpire, The RCC1 domain of Protein Associated with Myc (PAM) interacts with and regulates KCC2. *Cell Physiol Biochem* **22**, 31–44 (2008).

85. K. T. Kahle, J. Rinehart, P. de Los Heros, A. Louvi, P. Meade, N. Vazquez, S. C. Hebert, G. Gamba, I. Gimenez, R. P. Lifton, WNK3 modulates transport of Cl- in and out of cells: implications for control of cell volume and neuronal excitability. *Proc Natl Acad Sci U S A* **102**, 16783–16788 (2005).

86. J. S. Furyk, R. A. Meek, D. Egerton Warburton, Drugs for the treatment of nausea and vomiting in adults in the emergency department setting. *Cochrane Database Syst Rev* **2015**, CD010106 (2015).

87. M. Lau Moon Lin, P. D. Robinson, J. Flank, L. Sung, L. L. Dupuis, The Safety of Prochlorperazine in Children: A Systematic Review and Meta-Analysis. *Drug Saf* **39**, 509–516 (2016).

88. C. Ghelardini, N. Galeotti, C. Uslenghi, I. Grazioli, A. Bartolini, Prochlorperazine induces central antinociception mediated by the muscarinic system. *Pharmacological Research* **50**, 351–358 (2004).

89. Y. Bozzi, E. Borrelli, The role of dopamine signaling in epileptogenesis. *Front Cell Neurosci* **7**, 157 (2013).

90. X. Chi, X. Li, Y. Chen, Y. Zhang, Q. Su, Q. Zhou, Cryo-EM structures of the full-length human KCC2 and KCC3 cation-chloride cotransporters. *Cell Res* **31**, 482–484 (2021).

91. Y. Xie, S. Chang, C. Zhao, F. Wang, S. Liu, J. Wang, E. Delpire, S. Ye, J. Guo, Structures and an activation mechanism of human potassium-chloride cotransporters. *Science Advances* **6**, eabc5883 (2020).

92. T. A. Chew, J. Zhang, L. Feng, High-Resolution Views and Transport Mechanisms of the NKCC1 and KCC Transporters. *J Mol Biol* **433**, 167056 (2021).

93. S. Zhang, J. Zhou, Y. Zhang, T. Liu, P. Friedel, W. Zhuo, S. Somasekharan, K. Roy, L. Zhang, Y. Liu, X. Meng, H. Deng, W. Zeng, G. Li, B. Forbush, M. Yang, The structural basis of function and regulation of neuronal cotransporters NKCC1 and KCC2. *Commun Biol* **4**, 1–15 (2021).

94. N. Ankri, P. Legendre, D. S. Faber, H. Korn, Automatic detection of spontaneous synaptic responses in central neurons. *J Neurosci Methods* **52**, 87–100 (1994).

Acknowledgments: We thank Liset M de la Prida for helpful discussions and critical reading of the manuscript. We also thank Gilles Huberfeld for advices and assistance with handling and recording human postoperative brain tissues, Sabine Lévi, Etienne Côme and Marianne Renner for training and advices with single particle tracking (SPT) recordings and data analysis, Valérie Crépel for advices on synaptoporin immunostaining, and the Imaging Facility of the Institut du Fer à Moulin for assistance with confocal imaging.

Funding:

Fondation pour la Recherche Médicale DEQ20140329539 (JCP)

Fondation pour la Recherche Médicale FDT202106013286 (FD)

Agence Nationale de la Recherche ERANET-Neuron ANR-16-NEU3-0006-02 (JCP)

Fondation Française pour la Recherche sur l'Epilepsie (JCP)

Federation pour la Recherche sur le Cerveau (JCP)

Sorbonne Université (FD, JB, CP)

INSERM (JCP)

The Poncer lab is affiliated with the C-BRAINS network, supported by the Conseil Régional d'Ile de France.

Author contributions:

Conceptualization: FD, JCP

Formal Analysis: FD, AZ, JB, YK, CP, ND

Funding acquisition: JCP

Investigation: FD, AZ, JB, CP

Methodology: FD, AZ, JCP

Resources: MR, FB, BD, BM, VN, FC

Software: FD, YK, ND

Supervision: JCP

Visualization: FD, JCP

Writing – original draft: FD, JCP

Writing – review & editing: FD, JCP

Conflict of interest statement: JCP, FD and ZA are co-inventors on the patent: Methods and Pharmaceutical Compositions for Treating Refractory Epilepsy. WO2022219021. 2022 October. All other authors declare that they have no competing interests.

Data and materials availability: All data are available in the main text or the supplementary materials.

Abbreviations:

CCCs	cation-chloride cotransporters
CNS	central nervous system
DMSO	dimethylsulfoxide

D2R	dopamine receptor D2
ECoG	electrocorticography
FDA	Food and Drug Administration
GABA	γ-Aminobutyric acid
HFOs	high-frequency oscillations
HS	hippocampal sclerosis
ILAE	International League Against Epilepsy
KCC2	K/Cl cotransporter 2
IID	interictal discharge
IILDs	interictal-like discharges
MEA	multi-electrode arrays
mIPSCs	miniature inhibitory postsynaptic currents
mTLE	mesial temporal lobe epilepsy
NKCC1	N/K/Cl cotransporter 1
OSR1	oxidative stress-responsive kinase 1
PCPZ	prochlorperazine
SE	status epilepticus
SPAK	SPS1-related proline/alanine-rich kinase
WNK	with-no-lysine kinase

Tables and figures:

Patient ID	Neuropathology	Sex	Age at surgery	Age at seizure onset (years)	Seizure frequency	SEEG-video	Engel score	Medication	IILD-generating area (*in vitro*)
1	Hippocampal sclerosis, ILAE type 1	F	43	childhood (precise date unknown)	monthly	no	IC	LCS, LEV, LTG	undefined
2	Hippocampal sclerosis, ILAE type 1	F	49	11	weekly	no	IA	LCS, LEV	undefined
3	Hippocampal sclerosis, ILAE type 1	F	36	23	monthly	no	IA	LEV, OXC, PRP	DG, Sub.
4	Unconfirmed diagnosis of hippocampal sclerosis. Atrophy visible on MRI + malformation of cortical development.	F	37	18	monthly	yes	IV	LTG, ESC, CLB, ESCIT	DG, undefined
5	Hippocampal sclerosis, ILAE type 1	F	63	3	monthly	no	IA	CBZ, GBP, PB	undefined
6	Hippocampal sclerosis, ILAE type 3	M	58	40	monthly	no	ID	CBZ, LCS, CLB, R	DG, Sub.
7	Hippocampal sclerosis, ILAE type 1	F	16	12	monthly	yes	III	LEV, LTG	Sub. only
8	Hippocampal sclerosis, ILAE type 2	H	41	8	monthly	no	IC	LCS, LTG	Sub., undefined
9	No neuronal loss, ganglioglioma with BRAF mutation	F	45	20	weekly	yes	IA	TPM, PRP, CLB	DG, Sub.
10	Hippocampal sclerosis, ILAE type 1	H	37	29	weekly	yes	IA	ZNS, CBZ, LTG	undefined
11	Hippocampal sclerosis, not classifiable	F	32	12	monthly	yes	IIIA	LTG, PRP, TAC, AZT, EPZ, NVL, PRED, MEL	DG, Sub.
12	Hippocampal sclerosis, ILAE type 1	F	22	12	weekly	no	ID	CBZ, LCS, LTG, PRP	DG only
13	Hippocampal sclerosis, ILAE type 2	H	54	12-13	weekly	yes	IA	CBZ, TPM, ZNS	DG only

Table 1. Clinical, neuropathological and pharmacological features of the patient cohort. Abbreviations: AZT: Azathioprine; CBZ: Carbamazepine; CLB: Clobazam; ESCIT:

Escitalopram; ESC: Eslicarbazepine; EPZ: Esomeprazole; GBP: Gabapentine; LCS: Lacosamide; LTG: Lamotrigine; LEV: Levetiracetam; MEL: Melatonine; NVL: Nebivolol; OXC: Oxcarbazepine; PRP: Perampanel; PB: Phenobarbital; PRED: Prednisone; R: Ropinirole; TAC: Tacrolimus; TPM: Topimarate; ZNS: Zonesamide. DG: Dentate gyrus. Sub.: subiculum. Grey background indicates patients for which no significant effect of PCPZ or CLP257 on interictal-like activity was observed *in vitro*.

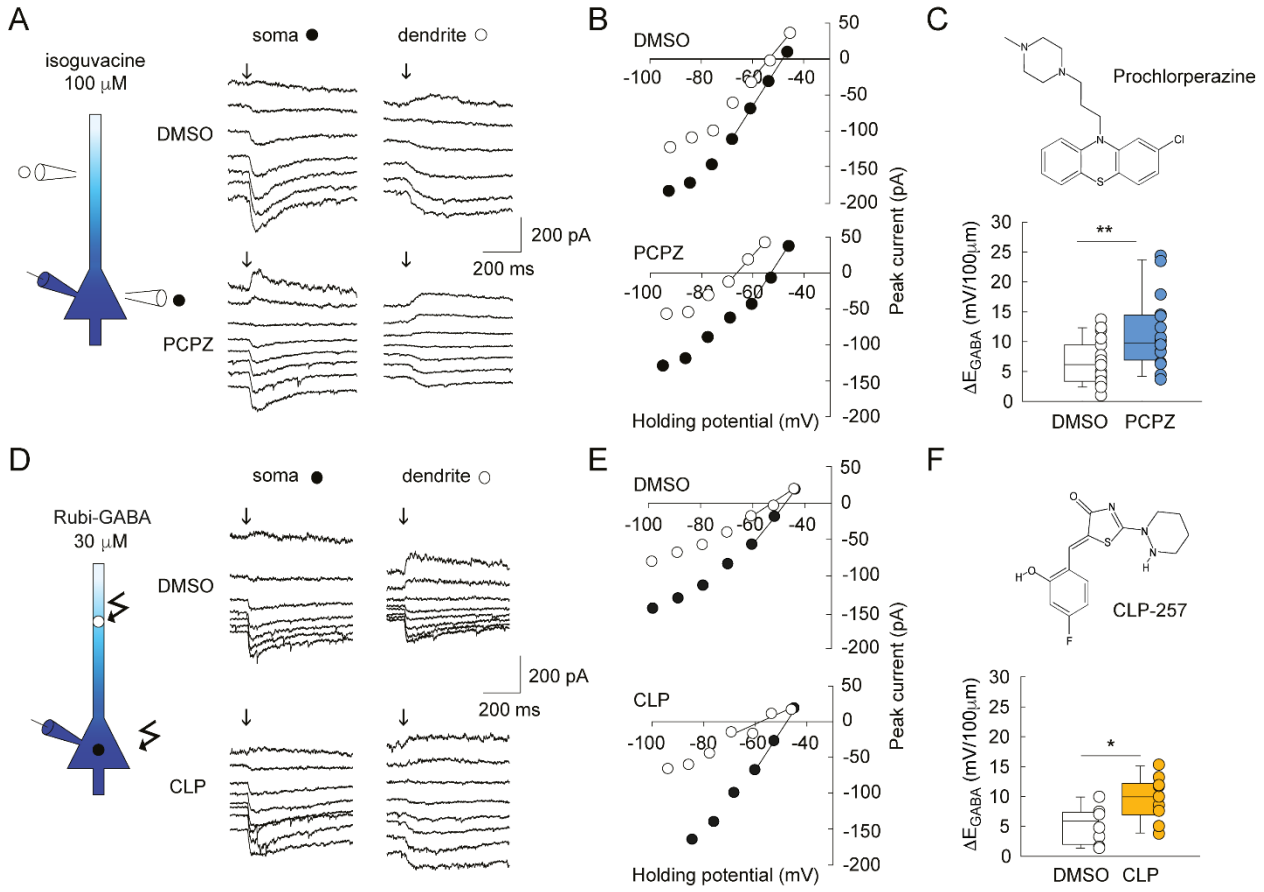

Fig. 1. Prochlorperazine (PCPZ) and CLP-257 promote chloride extrusion in hippocampal neurons. (A) Representative currents evoked at varying potentials by focal application of isoguvacine (arrow, 100 µM) onto the soma or dendrite of hippocampal neurons (21-24 DIV) previously treated for 2 hours with either vehicle only (DMSO, control) or PCPZ (10 µM). (**B)** I-V curves corresponding to the traces shown in A. (**C)** 2D chemical structure of PCPZ (top) and summary graph showing somato-dendritic E_{GABA} gradient (bottom, ΔE_{GABA}) in control and PCPZ-treated neurons (n=19 neurons and n=16 neurons respectively, from 5 independent cultures). ** t-test p<0.01. (**D-E**) same as in A-B, with currents evoked at varying potentials by focal uncaging of Rubi-GABA (arrow, 30 µM) onto the soma or dendrite of hippocampal

neurons, pretreated for 2 hours with either DMSO alone or 100 µM CLP-257 in DMSO. (**F)** 2D chemical structure of CLP-257 (top) and summary graph showing ΔE_{GABA} (bottom) in control and CLP-treated neurons (n=10 and 8 neurons, respectively, from 4 independent cultures) * t-test $p<0.05$.

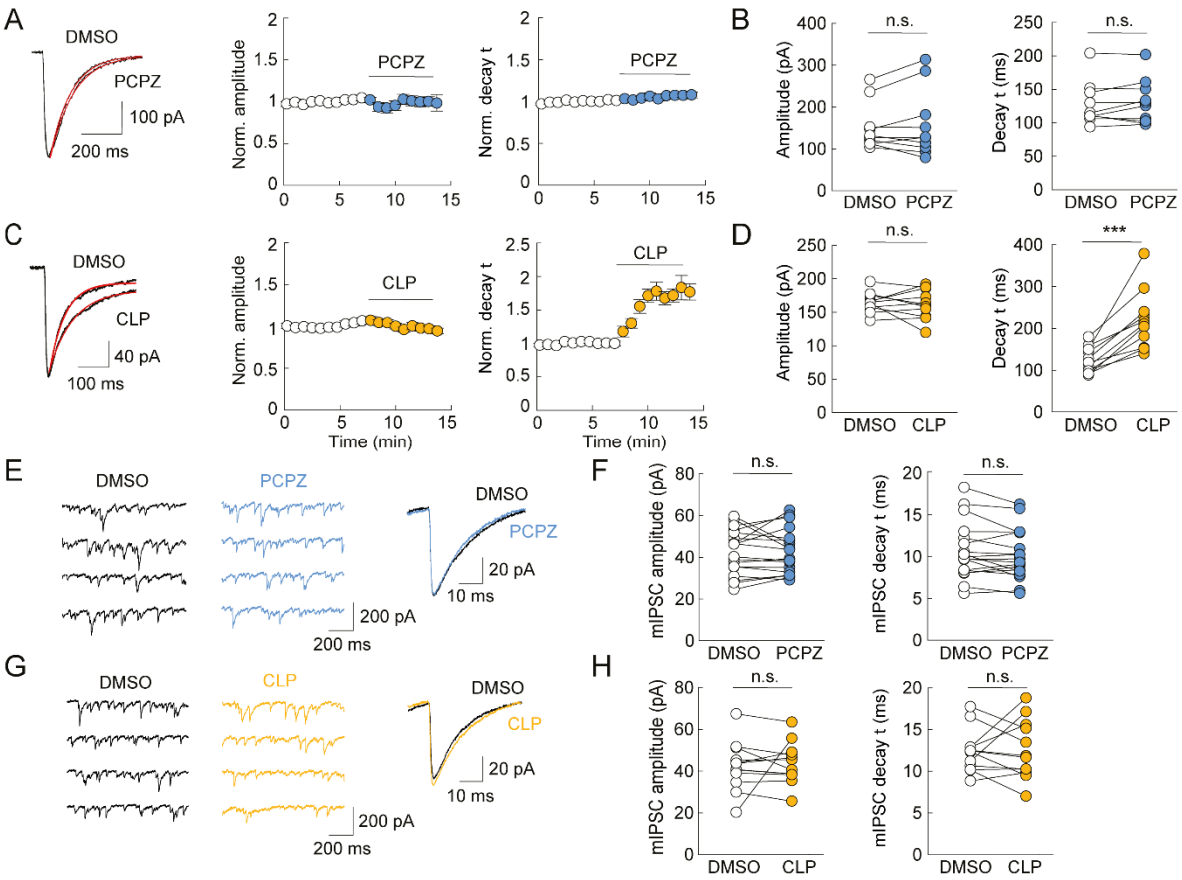

Fig. 2. CLP-257 but not PCPZ modulates $GABA_A$ receptor function. (A) Left, representative recording of currents evoked by focal somatic application of isoguvacine before and during acute application of 10 µM PCPZ. Evoked currents were averaged and their decay was fit with a simple exponential (red). Right, normalized amplitude and decay time constant over time of evoked currents. (**B)** Summary graphs showing the effect of PCPZ on the peak amplitude (left) and decay time constant (τ) of isoguvacine-evoked currents (n=10 neurons each from 2 independent cultures). (**C-D)** Same as in A-B for currents evoked by Rubi-GABA (30 µM) uncaging before and during application of 100 µM CLP-257 (n=11 neurons each from 2 independent cultures. *** Wilcoxon test, p<0.001). (**E**) Left, representative 5-seconds mIPSC

recording before (DMSO) and during application of PCPZ. Right, superimposed averaged mIPSCs detected from this recording. (**F**) Summary graphs showing the effect of PCPZ application on the amplitude (left) and decay time constant (right) of mIPSCs (n=18 neurons each from 4 independent cultures. *** Wilcoxon test, $p<0.001$). (**G-H)** same as E-F for CLP-257 showing no effect of CLP-257 on mIPSC amplitude and decay time constant (n=12 neurons each from 4 independent cultures. n.s.: not significant).

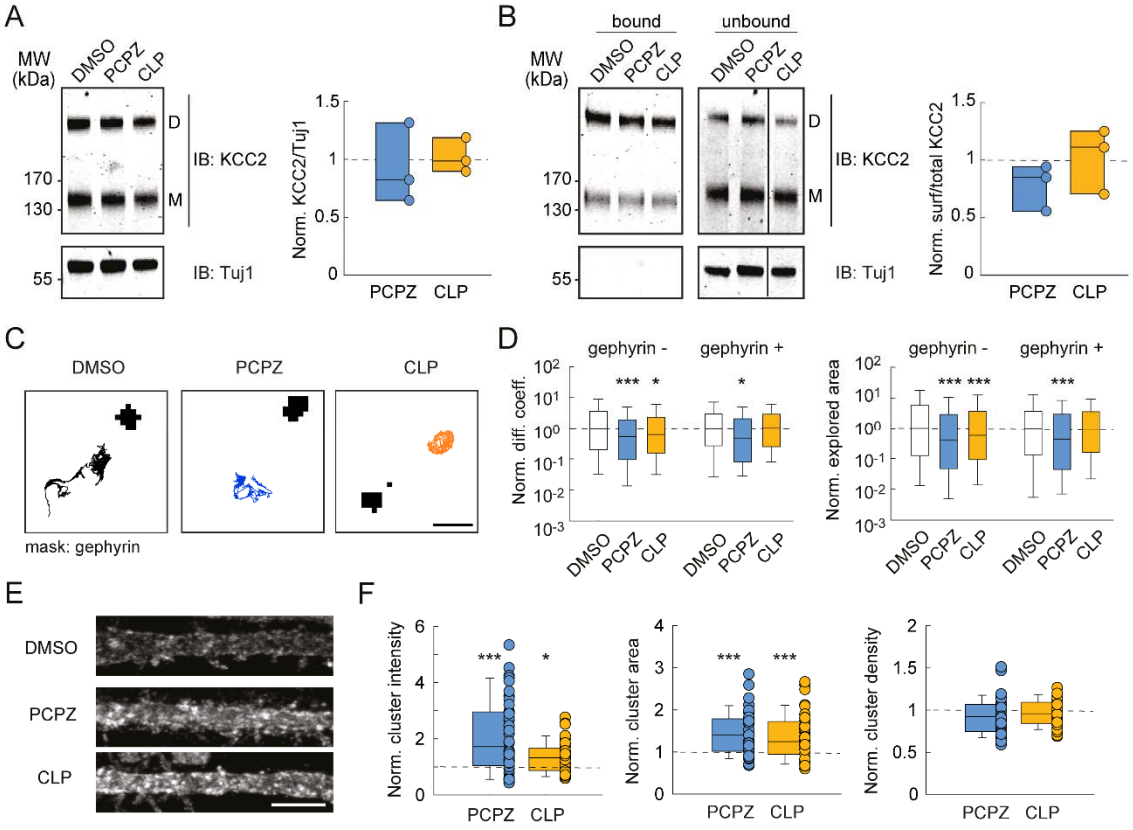

Fig. 3. Both PCPZ and CLP-257 reduce KCC2 membrane diffusion and promote its clustering in hippocampal neurons. (A) Left, representative immunoblots of protein extracts from primary hippocampal cultures treated for 2 hours with either PCPZ (10 µM), CLP-257 (100 µM) or DMSO alone. Right, quantification from 3 independent experiments. No significant change in total KCC2 expression was detected upon PCPZ or CLP-257 treatment as compared to control (t-test p=0.14 and p=0.89, respectively). **(B)** Representative immunoblots (left) and quantification (right) showing biotinylated surface KCC2 fraction (bound/total) was also unaffected upon PCPZ or CLP-257 treatment (n=3 independent cultures, t-test p=0.74 and 0.80, respectively). **(C)** Representative trajectories of recombinant KCC2 (black) outside inhibitory

synapses (gephyrin-FingR mask, grey), as detected using quantum dot-based single particle tracking, showing reduced lateral diffusion upon treatment with PCPZ or CLP-257. Scale, 1 µm. **(D)** Logarithmic distributions of median diffusion coefficients (D) and explored areas (EA) of KCC2 trajectories, outside (gephyrin -) or in the vicinity of (gephyrin +) inhibitory synapses, in control neurons (DMSO, D extra n=614, D syn n=162 and EA extra n=1836, EA syn n=486 quantum dots) and neurons treated for 2 hours with either PCPZ (D extra n=512, D syn=131 and EA extra n=1536, EA syn n=393 quantum dots) or CLP-257 (D extra n=697, D syn n=179 and EA extra n=2091, EA syn n=537 quantum dots). 4 independent cultures. Mann-Whitney test * $p<0.05$ *** $p<0.001$. **(E)** Maximum projections of confocal images of proximal dendrites after KCC2 immunostaining in cultured hippocampal neurons treated for 2 hours with PCPZ, CLP-257 or DMSO only. Scale, 5 µm. **(F)** Boxplots showing the distributions of integrated intensity, area and density of KCC2 clusters in control neurons and neurons exposed to either PCPZ or CLP-257. n=10 neurons per condition per culture and 4 independent cultures per condition. t-test or Mann-Whitney test * $p<0.05$ *** $p<0.001$.

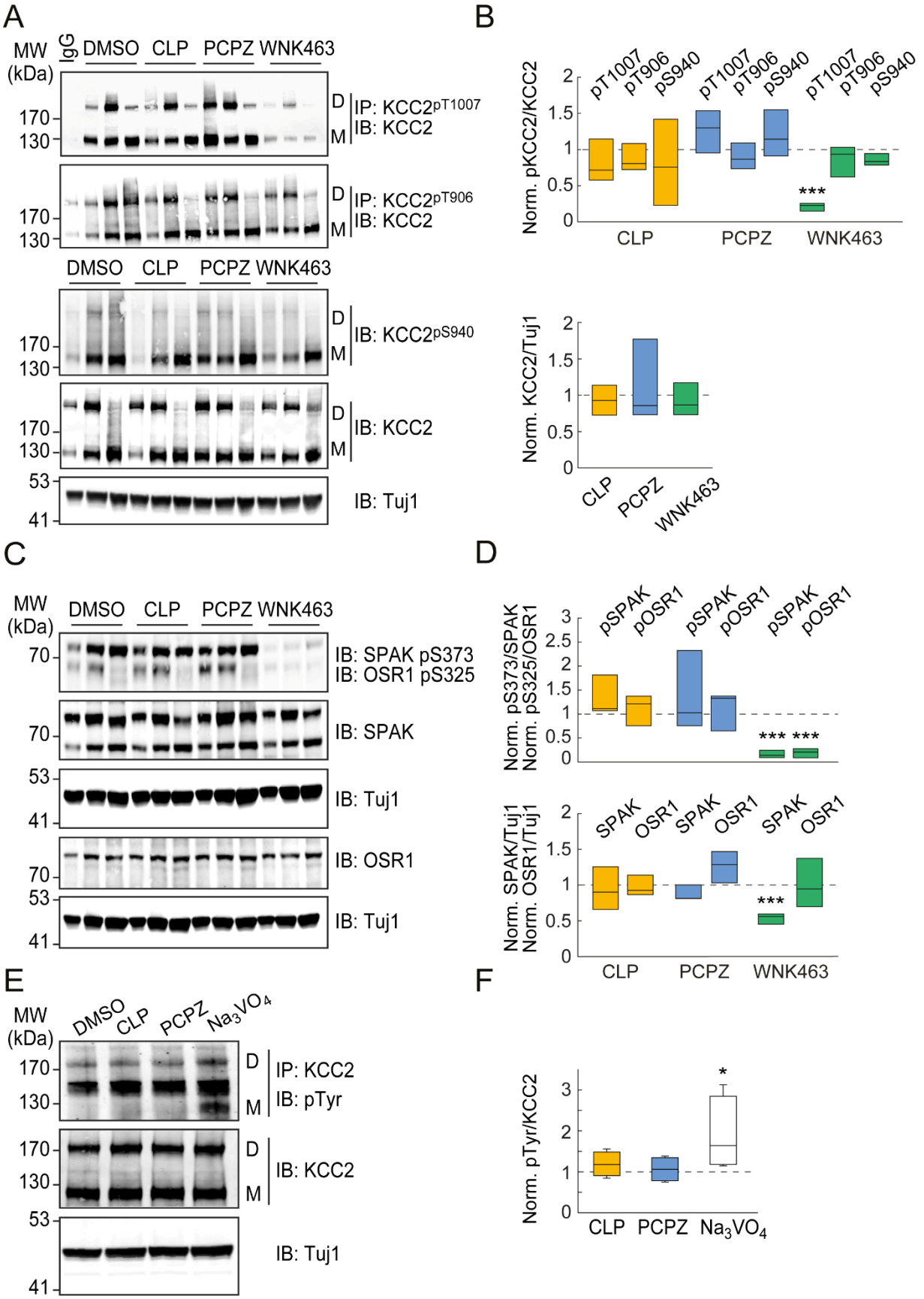
A
MW (kDa)
IgG
DMSO
CLP
PCPZ
WNK463
170
130
D
M
IP: KCC2pT1007
IB: KCC2
IP: KCC2pT906
IB: KCC2
IB: KCC2pS940
IB: KCC2
53
41
IB: Tuj1
B
Norm. pKCC2/KCC2
pT1007
pT906
pS940
***
CLP
PCPZ
WNK463
Norm. KCC2/Tuj1
C
70
IB: SPAK pS373
IB: OSR1 pS325
IB: SPAK
IB: Tuj1
IB: OSR1
D
Norm. pS373/SPAK
Norm. pS325/OSR1
pSPAK
pOSR1
Norm. SPAK/Tuj1
Norm. OSR1/Tuj1
SPAK
OSR1
E
Na3VO4
F
Norm. pTyr/KCC2
*

917

Fig. 4. PCPZ and CLP-257 do not affect phosphorylation of canonical KCC2 residues. (A) Immunoblots (IB) (left) of protein lysates or proteins immunoprecipitated (IP) with phosho-specific KCC2 antibodies, immunoblotted with antibodies against KCC2 or pS940 KCC2 and beta-tubulin (Tuj1) as control, prepared from hippocampo-cortical slices treated for 2 hours with either DMSO alone, CLP-257 (100 µM in DMSO), PCPZ (10 µM in DMSO), or the pan-WNK inhibitor WNK463 (10 µM in DMSO). IgG: control immunoglobulin G. (n=3 independent replicates 1-3). (**B)** Quantification from the 3 independent replicates shown in A. t-test ***$p<0.001$ (**C)** IB (left) of protein lysates, prepared as in A, immunoblotted with antibodies against SPAK, OSR1, or their phosphorylated forms and beta-tubulin (Tuj1) as control. (**D)** Quantification from the 3 independent replicates in B. t-test *** $p<0.001$. (**E)** Representative IB (left) of proteins immunoprecipitated with an anti-KCC2 antibody and immunoblotted with an anti-phosphotyrosine antibody, prepared from hippocampal-cortices slices treated for 2 hours with either DMSO, CLP-257 (100 µM in DMSO), PCPZ (10 µM in DMSO), or sodium orthovanadate (Na_3VO_4, 200 µM). (**F)** Quantification from the 4 independent replicates shown in E. Mann-Whitney test * $p<0.05$.

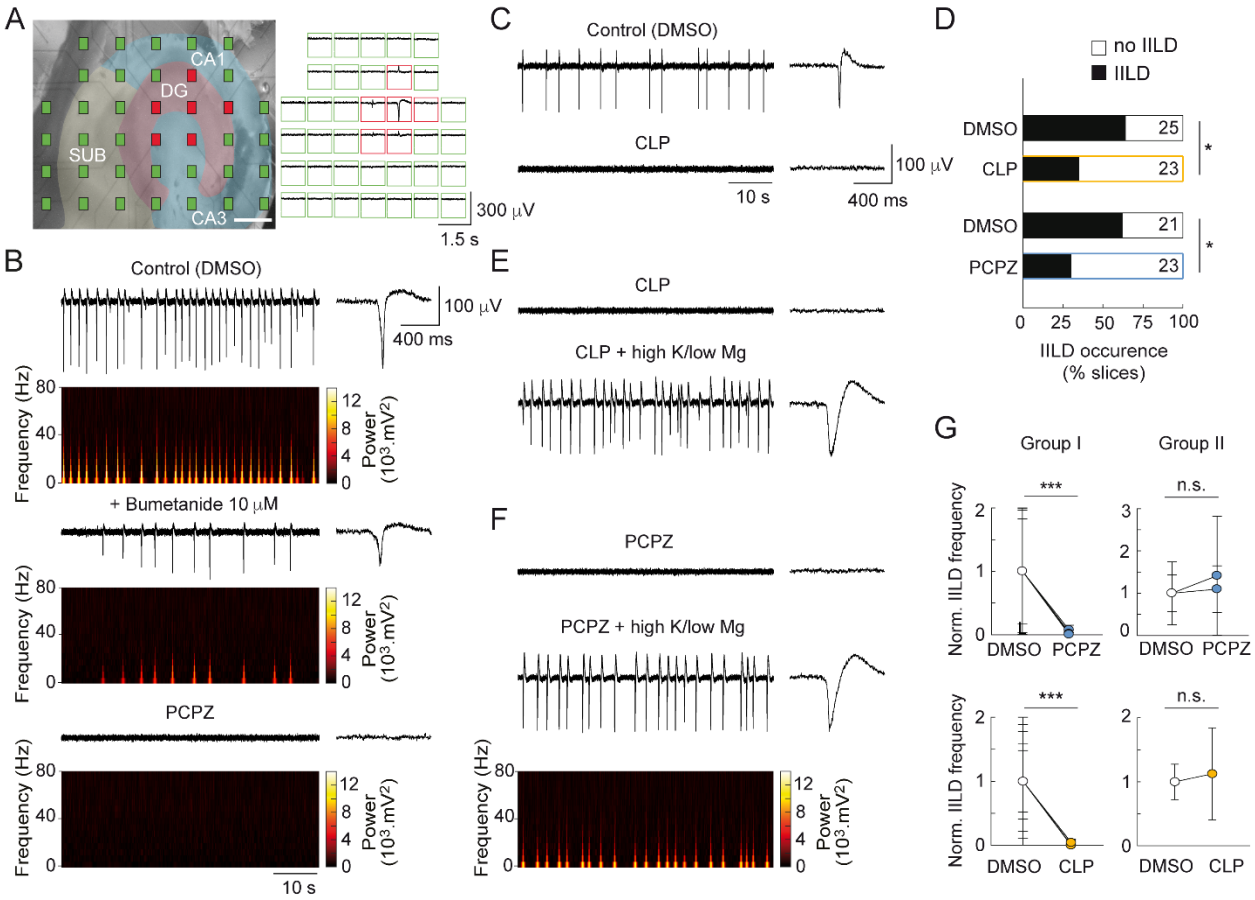

933

934 **Fig. 5. PCPZ and CLP-257 prevent spontaneous interictal-like discharges in temporal lobe**
935 **slices from mTLE patients. (A)** (Left) Photomicrograph of a recorded slice of resected brain
936 tissue from a mTLE patient, showing multielectrode array (MEA) layout. Hippocampal and
937 parahippocampal regions, including the subiculum, were delineated based on slice morphology.
938 Electrodes were color-coded to indicate the type of activity detected (red: interictal-like
939 discharges (IILDs) green: no activity). Scale: 1 mm. (Right) Representative recording from this
940 slice, showing synchronous IILDs mostly within the dentate gyrus. (**B)** Representative local field
941 potential recordings and spectrograms showing spontaneous, low-frequency (<40Hz) IILDs in a
942 slice maintained in control conditions (2 hours in DMSO only, top), and their reduction upon

>10 min application of 10 µM bumetanide (middle). These events were completely absent from an adjacent slice from the same tissue incubated for 2 hours in ACSF supplemented with 10 µM PCPZ (bottom). Insets show individual IILDs. (**C)** Representative recordings showing spontaneous IILDs in a slice from another patient incubated in control conditions (top), and the absence of these events in an adjacent slice kept for 2 hours in ACSF supplemented with 100 µM CLP-257 (bottom). (**D)** Summary plot showing the proportion of slices with and without IILDs. χ^2 test, * $p<0.05$. (**E-F**) Slices from two other patients treated with either CLP or PCPZ also did not display IILDs. However, application of a pro-convulsant ACSF (6.5 mM K^+ and 0.25 Mg^{2+}) rescued spontaneous IILDs in these slices. (**G)** Graphs showing the mean frequency of spontaneous IILDs (normalized to control) recorded in slices from 7 mTLE patients incubated in control ACSF (DMSO) or in the presence of 10 µM PCPZ. Two groups were distinguished: responders (Group I, 5 patients) and non-responders (Group II, 2 patients). Similar data are shown for slices from 6 patients, incubated in control ACSF or treated with 100 µM CLP-257. Wilcoxon signed rank test, *** $p<0.001$.

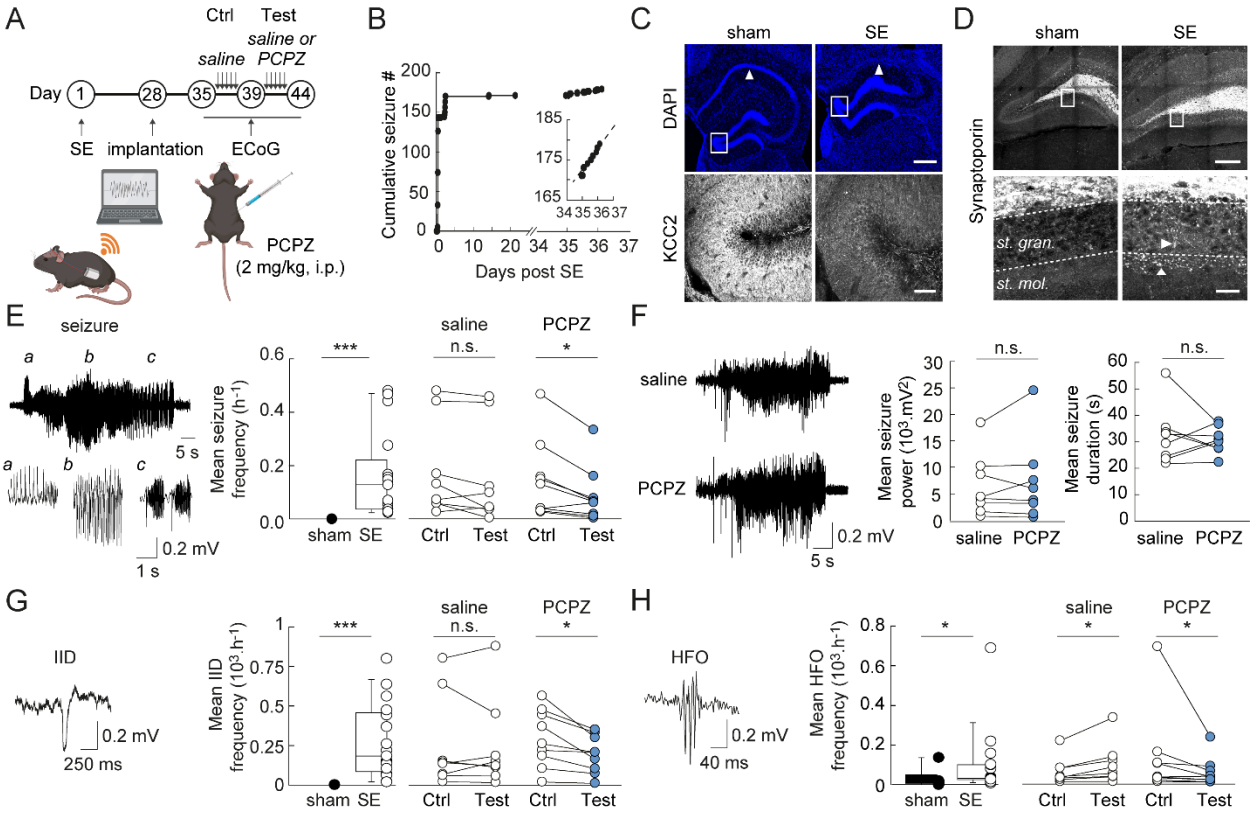

958

959 **Fig. 6. Chronic PCPZ administration reduces the occurrence of seizures and**
960 **epileptiform activities in a mTLE mouse model. (A)** Experimental timeline. (**B)** Graph
961 showing the cumulative number of seizures detected in a mouse immediately after SE and up to
962 37 days post SE. Recording was interrupted between days 21 and 34 post SE. Note that seizures
963 stop 2 days after SE and chronic seizures occur at a regular rate after day 34 (inset). (**C)** Top,
964 representative confocal fluorescent micrographs of DAPI staining of hippocampal slices from
965 naïve (no SE) and epileptic mice. Arrowheads indicate the CA1 region, which is largely sclerotic
966 in the epileptic mouse. Also note the dispersion of the dentate gyrus granule cells. Scale: 400
967 µm. Bottom, confocal fluorescent micrographs of KCC2 immunolabelling in dentate gyrus, from
968 the regions boxed in top panels, showing reduced KCC2 immunofluorescence in the dentate

gyrus of the epileptic mouse. Scale: 60 µm (**D)** Top, representative confocal fluorescent micrographs of synaptoporin immunolabelling of the dentate gyrus of control and epileptic mice. Scale: 200 µm. Bottom, magnification of the regions boxed in top panels, showing ectopic synaptoporin-immunopositive mossy fibers in the stratum granulosum and stratum moleculare only in the epileptic mouse. Scale: 20 µm. (**E)** Left, representative ECoG recording of a seizure with insets (a,b,c) showing typical periods of the seizure. Middle, summary graphs showing mean seizure frequency per hour in sham (no SE, n=6) and epileptic mice (n=17). No seizures were detected in sham animals (*** Mann-Whitney test $p<0.001$). Right, summary graphs showing mean seizure frequency per hour in epileptic mice receiving saline i.p. injections during the control period (days 35-39) and either saline or PCPZ during the test period (days 40-44). Mice receiving PCPZ injections during the test period displayed significantly less seizures than during the control period (n=9 mice, * paired t-test $p<0.05$), while no change in seizure frequency was observed in mice receiving saline injections (n=8, p=0.118). (**F**) Summary graphs comparing mean seizure power (left) and duration (right) during the control (saline) and test (PCPZ) periods. While reducing seizure frequency, PCPZ had no significant effect on seizure power (paired t-test p=0.466) or duration (p=0.657, n=8 mice). (**G-H)** Left, representative ECoG recording of an interictal discharge (IID, in G) and a high-frequency oscillation (HFO, in H). Middle, summary plots showing mean IID (in G) and HFO (in H) frequency in sham (n=6) and epileptic animals (n=17). IIDs and HFOs were significantly more frequent in epileptic animals (Mann-Whitney test * $p<0.05$, *** $p<0.001$, respectively). Right, summary plots of mean IID (in G) and HFO (in H) frequency during the control period (days 34-39) and the test period (days 40-44). Recordings from mice receiving PCPZ injections during the test period displayed

significantly reduced IID and HFO frequency as compared to the control period (* paired t-test $p<0.05$, n=9 mice). Recordings from mice receiving saline injections during the test period revealed no change in IID frequency ($p=0.846$) and a significant increase in HFO frequency (* $p<0.05$, n=8 mice).